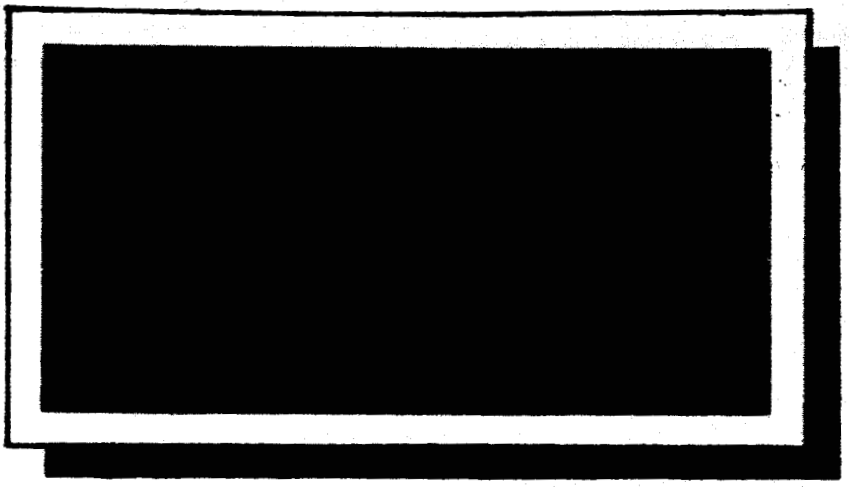

CENTER FOR SPACE RESEARCH

MASSACHUSETTS INSTITUTE OF TECHNOLOGY

SUNBLAZER STATE DETERMINATION INVESTIGATION

by

Dennis O. Madl

CSR T-66-4 May 1966

SUNBLAZER STATE DETERMINATION INVESTIGATION

by

Dennis Oscar Madl

Submitted to the Department of Aeronautics and Astronautics on 20 May, 1966, in partial fulfillment of the requirements for the degree of Master of Science.

ABSTRACT

Sunblazer is a small solar probe that will be tracked using signals received from an onboard transmitter. The measurable quantities are the azimuth and elevation angles of the probe and range-rate as inferred from a doppler frequency shift. These are measured in station coordinates at a single receiving station. A filter is developed for recursively estimating the probe state. The quality of the estimation procedure is investigated by computing the correlation matrix of estimation errors at probe conjunction, so that the sensitivity of the estimation uncertainties to uncertainties in range-rate data are determined. It is found that the estimation uncertainties of 4 of the 6 state components can be reduced to 20% of the value calculated without range-rate data. This requires that the residual frequency uncertainties, which are primarily a function of the onboard transmitter, be reduced to 1 part per 10^8. To achieve this, a second filter is developed for reducing short term frequency variations to a low level. Methods are also suggested for estimating the longer term transmitter drift.

Thesis Supervisor: John V. Harrington

Title: Professor of Aeronautics and Astronautics; and Director, Center for Space Research

ACKNOWLEDGEMENTS

The author wishes to express his appreciation and thanks to: Professor John V. Harrington for suggesting this study and for his guidance, to Mr. John H. Fagan and Mr. William T. McDonald and other staff members of the Experimental Astronomy Laboratory and the Center for Space Research for their helpful advice and suggestions, and to Miss Martha Idell for the conscientious effort she devoted to the typing to this thesis. The author also wishes to thank the Experimental Astronomy Laboratory for supplying the computer time necessary for this analysis.

The author wishes to thank the Department of the Air Force and the Air Force Institute of Technology for providing the opportunity for graduate study at the Massachusetts Institute of Technology.

TABLE OF CONTENTS

TABLE OF CONTENTS (continued)

TABLE OF CONTENTS (continued)

SYMBOLS

$\underline{(\ )}$	quantity ( ) is a vector
$\overline{(\ )}$	mean value of quantity in ( )
$(\ )'$	quantity ( ) has been updated from a prior time with the state transition matrix
$\hat{(\ )}$	quantity ( ) is a maximum likelihood estimate
$\tilde{(\ )}$	quantity ( ) is a measured value
$\underline{(\ )}_3$	first three components of a 6 dimensional vector
$\underline{0}_3$	the last three components of a 6 dimensional vector, which are zero.
$(\ )_N$	a nominal value
$\underline{1}_X$	unit vector along X axis
tr( )	the trace of the matrix ( ), where ( ) is square
$(\ )^T$	the transpose of the matrix or vector ( )
$(\ )^{-1}$	the inverse of the square matrix ( )
A	azimuth angle
L	elevation angle
$\dot{\rho}$	earth-probe range-rate
α	measurement error associated with azimuth angle
β	measurement error associated with elevation angle
γ	measurement error associated with range-rate
$\delta(\ )$	deviation in ( ) from a nominal value
Δf_B	frequency shift due to Brillouin scattering
$\underline{a}$	measurement vector associated with azimuth angle in the xyz frame
$\underline{k}$	measurement vector associated with azimuth angle in the pqu frame

$\underline{b}$	measurement vector associated with elevation angle in the xyz frame
$\underline{d}$	measurement vector associated with elevation angle in pqu frame
$\underline{c}$	measurement vector associated with range-rate
$\underline{h}$	general measurement vector
$\underline{e}$	error in estimate of the state deviation vector
$\underline{\mu}$	vector of measurement errors, $[\alpha \ \beta \ \gamma]^T$
Ψ	flight-path angle
ϕ	angle between x axis and p axis, except in Chapter 2 it is the scattering angle
ϕ_o	the standard deviation of the scattering angle
λ	angle between X axix and p axis, except in Chapter 2 it is wavelength in meters
Θ	the angle of refraction caused by passage of the signal through the corona
σ	standard deviation
c	the speed of light
a,e,i	semi-major axis, eccentricity, and inclination angle of an ellipse, except that a subscript h indicates the same elements for an hyperbolic trajectory
f	true anomal
$\underline{H}$	angular momentum
M	rotation matrix (3 x 3)
Φ	state transition matrix (6 x 6)
E	error covariance matrix (6 x 6)
A	correlation matrix of measurement errors (3 x 3)
W^o	optimum filter (6 x 3)
H	matrix made up of measurement vectors $\underline{k}^T \ \underline{d}^T \ \underline{c}^T$ (3 x 6)
r	magnitude of sun-earth radius, except in Chapter 2 it is the solar radius

v	magnitude of earth's velocity
v_m	the radial velocity of gases in the solar corona
R	magnitude of sun-probe radius
V	magnitude of probe velocity
$\lvert(\_)\rvert$	the magnitude of the vector (_)

SUBSCRIPTS

n,n-1,c	refer to time (t_n), a prior time (t_{n-1}), and time of conjunction
xyz	vector is written in components of xyz frame
pqu	vector is written in components of pqu frame
XYZ	vector is written in components of XYZ frame
bo	refers to burnout
SOI	refers to quantity at the earth's sphere of influence
e	refers to earth
s	refers to sun
h	refers to hyperbolic trajectory
1	in Chapter 2 refers to the 75 Mc/sec signal
2	in Chapter 2 refers to the 225 Mc/sec signal

QUANTITIES

r_{SOI}	574,000 miles
r	1 AU
μ_e	14.07528×10^{15} ft^3/sec^2
μ_s	$\mu_e / 3 \times 10^{-6}$
r_e	20.88×10^6 ft
1 AU	92.9×10^6 miles

CHAPTER 1

THE PROBLEM AND THE RESULTS

1.1 General Statement of the Problem

Sunblazer is a small, relatively low cost space probe. The first probe is to be placed into solar orbit in an effort to determine some properties of the solar corona. The possibility also exists of using similar probes for other deep space missions. The probe contains a transmitter that transmits signals which will be received at a ground station. Certain characteristics of this signal are to be used to track the probe. For the probe considered here, these characteristics are the azimuth and elevation angle of the signal in a station fixed coordinate system, with the possibility of range-rate data inferred from doppler frequency shift. The problem considered here is estimation of the probe state (i.e., the six components of probe position and velocity) in the face of measurements which are corrupted with errors. More specifically, this paper investigates the estimation problem to determine methods of processing the available data to obtain an optimum state estimation. The ability to measure the azimuth and elevation angles is assumed to be unalterable. Doppler frequency shift can supply range-rate data. However, our ability to determine a frequency shift is limited by our ability to pin down error sources such as drift in the transmitter and ionospheric frequency shifts, as well as our ability to detect frequency shifts. Using angular data only, it is possible to estimate the probe state to within certain limits of uncertainty. If it is properly incorporated into the estimation procedure, the addition of range-rate data, even if poorly known (in a statistical sense) must reduce this uncertainty. However, the sensitivity of the estimation procedure to the uncertainty of the frequency errors, especially transmitter drift, was not

initially known. Because of this, it was not obvious which error sources could be neglected or how well the transmitted frequency needed to be known to gain any given reduction in uncertainty in state estimation. The problem considered here, then, is how well probe state can be estimated through application of filtering techniques to range-rate as well as angular data.

1.2 The Approach to the Problem

a) Assumptions

The purpose of the analysis was to determine the improvement in estimation of probe state gained by using range-rate data. The Sunblazer probe considered here is designed to determine more accurately the electron density of the solar corona. The effects of the corona on an electromagnetic wave passing through it are not known accurately enough to use the data effectively for state estimation. While it is possible to formulate the problem in such a way that both the effects of the corona and the state can be estimated, it was decided that it would be easier conceptually to discontinue the filtering of data for the purpose of state estimation, and to use prediction techniques, during that period when the effects of the corona are appreciable but not well known. It was decided (see Chapter 2.3) to discontinue filtering for two weeks on each side of conjunction. For the remainder of the mission, data is to be filtered to obtain the estimate of probe state.

The nominal trajectory of the probe will be close to a two-body ellipse around the sun, and the center of the earth is almost in circular orbit around the sun. Consequently, it is not detrimental to the results of this analysis to assume as models,an elliptical orbit for the probe and a circular orbit for the earth, as long as it is recognized that in applying this analysis to an actual probe the true trajectories of the probe and the earth would need to be used to get comparable results.

In this analysis, it is assumed that the measurements of azimuth angle, elevation angle, and range-rate are made from a receiving station at the center of the earth. The azimuth and elevation angles as measured from the actual ground station define the direction of the probe. These angles are assumed to be normally distributed about the true value with standard deviations of $1/10^{\circ}$. If the actual ground

station location is known exactly, the direction of the probe can be transformed from station coordinates to any desired earth-centered coordinate system, where a new azimuth and elevation angle can be defined to give the direction of the probe in the earth-centered coordinate system. In this analysis it is assumed that this has been done, and that the statistical properties of these new angles are unchanged; that is, the new azimuth and elevation angles are normally distributed about the true values and have standard deviations of $1/10^{o}$.

Probe-ground station range-rate is the projection of total probe velocity on the probe-ground station line. On the other hand, range-rate as measured from the hypothetical earth-centered station is the projection of total probe velocity on the line from the center of the earth to the probe. These two directions, in general, are not parallel. Because the ground station does not measure probe velocity components in the plane perpendicular to the probe-ground station line, there is not enough information available to actually effect a transformation of station-measured range-rate to the non-parallel range line from the center of the earth. If the probe is at any appreciable distance from the earth, the difference in range-rate as seen along these non-parallel lines will be small. Consequently, the analysis presented here and the conclusions drawn from it will not be adversely affected. However, the difference may be large enough that in processing data for a real mission the analysis will need to be altered to account for this difference.

It is assumed that the transmitted frequency is composed of two parts. The first part is a mean frequency that may vary slowly with time due to long term oscillator drift. The second part is a residual uncertainty that is normally distributed with a given standard deviation. In this analysis, the standard deviation is used as an independent variable. (explained in Chapter 1. 2b) It is assumed that the residual uncertainties are short term phenomena, and that their correlation time

is very small compared to any sampling period. It is also assumed that the long-term drift is either a known function of time (deterministic) or can be estimated so well that it can be considered deterministic compared to any residual uncertainties.

b) The Method of Attack

The method of attacking the problem was to assume range-rate of varying quality to determine the sensitivity of the estimation uncertainty to the uncertainty in range-rate data. Specifically, it was assumed that the error sources and residual frequency uncertainties caused the range-rate data to be a random process, normally distributed about the true value and having a standard deviation of $\sigma_{\dot{\rho}}$, which was assigned various values. To form a basis for comparison, a figure of merit was devised. This figure of merit is the uncertainty in the estimate of each of the six components of the state vector at the time of conjunction. The uncertainties in the estimate were then computed for a set of range-rate standard deviations. The results are then interpreted in terms of error sources that must be considered, and the level of knowledge of transmitter drift required, to obtain range-rate data of the quality needed to achieve a given amount of reduction in the estimation uncertainties. Finally, some suggestions are offered for determining the transmitter drift to the required accuracy.

1.3 The Results

The analysis presented here was carried out for a probe having an elliptic nominal orbit lying in the ecliptic plane and having a period of 2/3 year. (The nominal trajectory is described in greater detail in Chapter 2.) A filter is developed that will recursively estimate state deviations from the nominal when data from an actual probe are available. The uncertainties in this state estimation process have also been determined, so that the quality of the estimation procedure has been evaluated using the statistics of the anticipated errors in the data to be measured. The total number of measurement times was chosen as 30, and 3 measurements (azimuth, elevation angle, and range-rate) are made at each measurement time.

The assumption that the measurement errors are normally distributed causes the estimation error in each of the 6 state components to be normally distributed. The matrix **E** is the correlation matrix of

these estimation errors, (also termed the error covariance matrix) and the diagonal elements are the statistical variances of the 6 components. The error covariance matrix at conjunction, E_c, is calculated using range-rate data of varying quality. The square-root of each variance (i.e., the standard deviation) is used as a measure of the uncertainty in estimate of the corresponding state component. These standard deviations are functions of the quality of range-rate data used. The results of the computations made are presented in graphical form in Figures 1.1 and 1.2 and again in tabular form in Table 5.1.

It is apparent from these graphs that the uncertainties in the estimation of the out-of-plane components of probe state are insensitive to the quality of the range-rate data. The direct cause of this is the fact that nominal probe orbit was assumed to be in the ecliptic plane. Consequently, only elevation angle measurements yield information about the out-of-plane components, and the standard deviation of the elevation angle errors is assumed to be fixed at $1/10^{o}$. The out-of-plane position uncertainty is relatively good compared to the in-plane position uncertainties discussed below for a residual frequency uncertainty of 3/4 cps. The velocity uncertainty is not as good. However, if a nominal trajectory with an inclination to the ecliptic is selected, range-rate information in the out-of-plane direction will be available and should help reduce the out-of-plane estimation uncertainties, especially the velocity uncertainty. On the other hand, range-rate data permits the uncertainties in the in-plane components to be reduced to less than $20^{o}/o$ of the uncertainties when only angular data are filtered to obtain a state estimate. To reduce the uncertainties to this level, it is necessary to reduce the residual frequency uncertainties to 3/4 cps (based on a transmitted frequency of 75 Mc/sec). The method suggested for doing this is to take an average of 400 samples of apparent doppler shift (corrected for transmitter drift and relativistic effects) taken at 10 second intervals for 67 minutes. This average is used as an estimator of the true doppler shift due to range-rate. Effectively, then, the problem has been separated into two distinct filtering problems. The first is to occur for 67 minutes daily to reduce residual frequency uncertainties to a low level. The other filtering occurs once daily on the measured azimuth, elevation angle,

and range-rate data to estimate the probe state recursively.

To obtain an estimate that is this good, long term frequency drift must be well known. To determine this drift, it is suggested that a transmitter model with an unknown, but constant, parameter be hypothesized.

$$f(t) = 75\,\text{Mc/sec}\,[1 + a\,t] \tag{1.1}$$

where the parameter "a" is the drift rate. The state vector is then expanded to 7 components. The problem then must be reformulated in such a way that the measurements are processed with a new filter to estimate the deviations in position and velocity and the model parameter, "a." This analysis was not carried out and is suggested as possible extension of this study.

These results and conclusions are discussed in greater detail in Chapter 5, and the problem of state estimation and calculation of the error covariance matrix at conjunction are covered in Chapter 4.

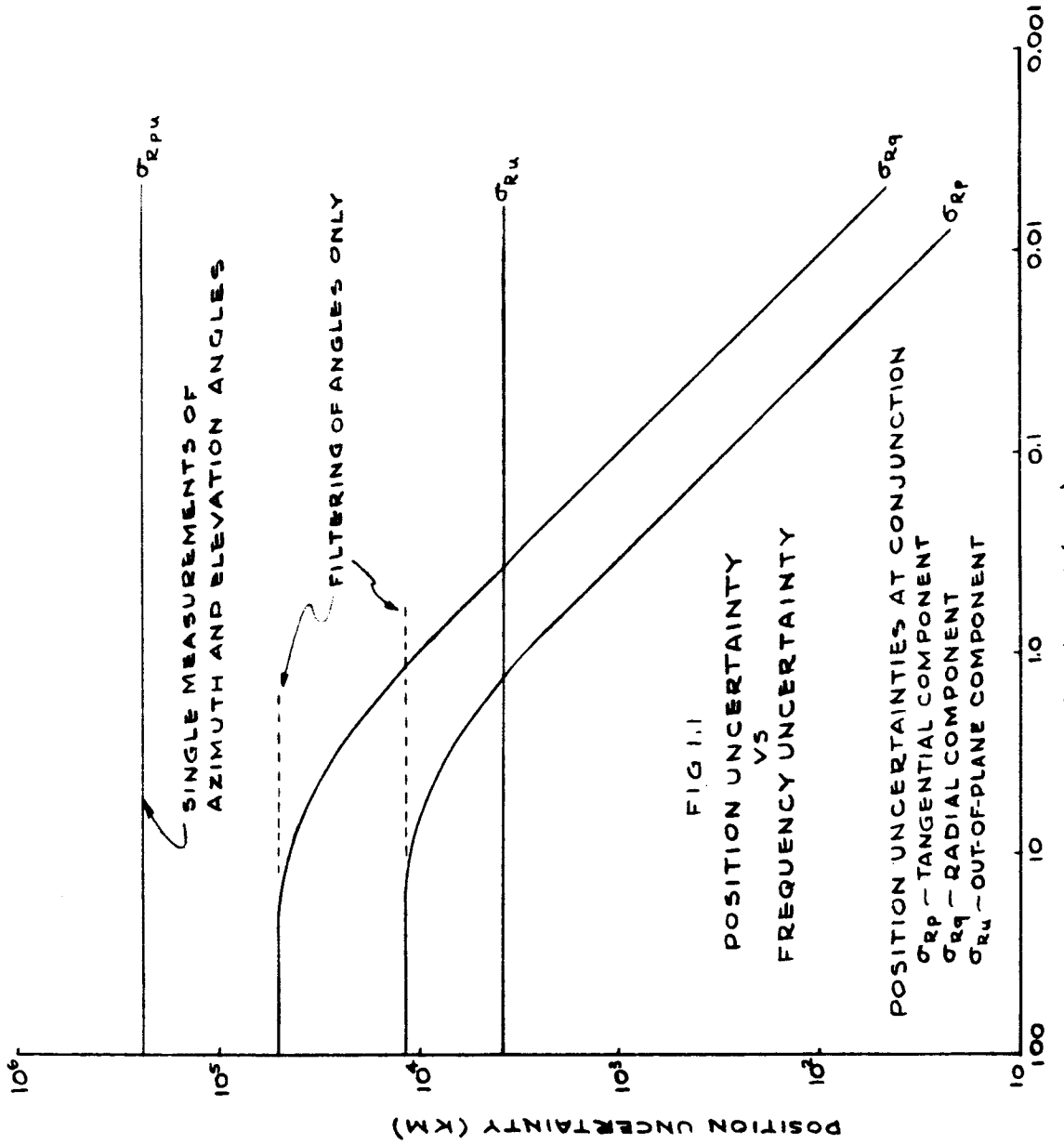

FIG 1.1
POSITION UNCERTAINTY
VS
FREQUENCY UNCERTAINTY

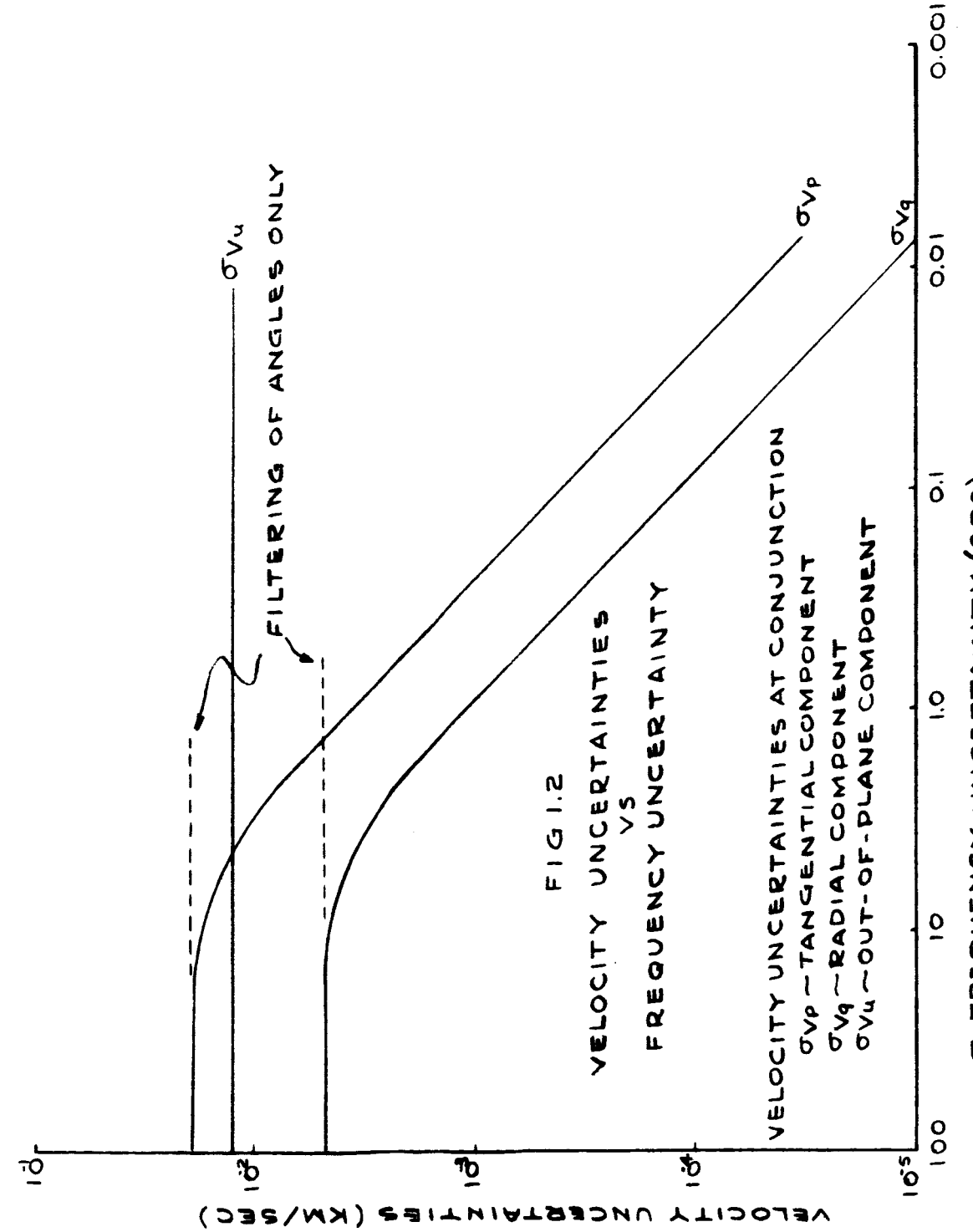

FIG 1.2
VELOCITY UNCERTAINTIES
VS
FREQUENCY UNCERTAINTY

CHAPTER 2

SYSTEM ERRORS AND ASSUMPTIONS

The Sunblazer probe considered here is a lightweight solar probe that will undergo superior conjunction one year after launch. The probe will have on board a transponder and a transmitter that broadcasts at two frequencies, a primary frequency of about 75 Mc/sec, and a secondary frequency of exactly three times the primary frequency. The receiving station will be located at El Campo, Texas, and can measure the azimuth and elevation angles of an incoming signal in a station fixed coordinate system. At some time period during the mission the transmission path will pass through the solar corona. All signals will pass through the atmosphere and the ionosphere. The nature and size of errors inherent in the equipment and some basic assumptions are considered in this chapter.

2.1 The Transponder

The probe carries a transponder designed to operate for one to two weeks. Consequently, it can supply range, range-rate, and angular data during the early phase of the mission. However, it is assumed that the nominal trajectory (to be defined later) will be sufficient for the purposes of this analysis. Consequently, transponder errors are not considered here, although a possible use of the transponder is discussed in Chapter 5.

2.2 Angular Data

The receiving station for this project is at El Campo, Texas. It is assumed that the station location is known exactly, so that angular data received at the station can be transformed to the center of the earth with no errors except those made in measuring the azimuth and elevation angles at the receiving station. A phased array antenna will be used to determine these angles. It is assumed that

the errors in the angles measured at the station form an unbiased normal distribution about the true values. Based upon the expected accuracy of the El Campo antenna, the standard deviations of the angular measurements are taken to be $1/10^{o}$. It is assumed that these angles can be transformed to the center of the earth to give azimuth and elevation angles (shown in Figure B.1) that have unchanged statistical properties.

2.3 Effects of the Solar Corona

One of the goals of the probe considered here is to determine the electron density of the solar corona, which is not very well known. Theoretical results and some experiments using star occultations give a clue to the magnitude of the effects on electromagnetic radiation passing through the corona. Three of the effects are refraction, scintillation, and frequency shift due to Brillouin scattering. It is possible to formulate the estimation problem in such a way that data can be filtered to obtain an estimate of both probe state and the effects of the corona. However, for reasons of conceptual and analytical simplicity, the approach will be to filter data to estimate the state until the effects of the corona become significant. During the period of significant corona effects, prediction techniques will be used to estimate spacecraft state. During the prediction, received data will be available for determining the corona's electron density, which is not done in this analysis.

a) Refraction

An electromagnetic wave passing through a low pressure, moving gas is, based upon an Allen Baumbach model of the corona (8:26), refracted by an amount Θ, where

$$\Theta = \frac{76\lambda^2}{r^3} \tag{2.1}$$

Here, Θ is the refraction angle in minutes of arc, λ is the wavelength in meters, and r is the displacement (from the sun) of the transmission path in solar radii. For our problem,

$$\Theta_1 = \frac{1216}{r^3} \tag{2.2a}$$

$$\Theta_2 = \frac{1}{9}\Theta_1 \tag{2.2b}$$

where Θ_1 is the angle of refraction for the primary signal (75 Mc/sec). A graph of approximate refraction angles as a function of r is shown in Figure 2.1. If the path displacement is greater than 25 solar radii, ignoring refraction in the corona will not appreciably effect the accuracy of the state estimation procedure, because the refraction angle will be much smaller than $1/10^{o}$.

b) Scintillation

Electromagnetic waves passing through a turbulent refractive medium are scattered about a median ray (which has already been refracted through an angle Θ). The arriving, scattered waves are assumed to have a normal angular distribution about the median ray (8:25). The standard deviation of the scattering angle, σ_{ϕ}, is given by

$$\sigma_{\phi} = \phi_o = \frac{K\lambda^2}{r^n} \tag{2.3}$$

where K and n have been empirically determined to be

$$11 < K < 50 \tag{2.4a}$$

$$1.2 < n < 2.2 \tag{2.4b}$$

Picking K and n to give the largest standard deviation yields

$$\phi_{o,1} = \frac{800}{r^{1.3}} \tag{2.5a}$$

$$\phi_{o,2} = \frac{1}{9}\phi_{o,1} \tag{2.5b}$$

A graph of ϕ_o as a function of r is shown in Figure 2.2. Scintillation itself contributes no direct error. It may create a problem in detection of the signal if ϕ_o is too large compared to the beam width of the antenna. The beam width of the antenna is sufficiently large compared to ϕ_o that, except for displacements of the transmission path of less than three or four solar radii, signal detection is possible.

c) Frequency Shift

At very low gas pressures the thermal velocity of molecules can produce a doppler effect. (5:10-21) In the sun's corona, this doppler shift is due to Brillouin scattering of the wave. It is found that (Ref. 14)

$$\frac{\Delta f_B}{f} = 2 \sin^2 \frac{\Theta}{2} (v_m/c) \tag{2.6}$$

where Δf_B is the frequency shift due to Brillouin scattering, Θ is the angle of refraction, c is the speed of light, and v_m is the radial ve-

locity of the low pressure gases in the solar corona. Assuming Θ is a small angle measured in radians, we find that

$$\Delta f_{B,1} = \frac{5 \times 10^6}{r^6} \ (^v m/c) \text{ cps} \tag{2.7a}$$

$$\Delta f_{B,2} = \frac{1.9}{r^6} \times 10^5 \ (^v m/c) \text{ cps} \tag{2.7b}$$

The ratio $^v m/c$ cannot possibly exceed one, and is more likely to be on the order of 10^{-3}. It would appear that, for purposes of state estimation, this frequency shift can be neglected for transmission paths displaced from the sun by more than 10 solar radii.

d) Summary

Based upon the above analysis, the errors caused by neglecting the effects of the corona can be safely assumed to be negligible for transmission path displacements greater than 50 solar radii. This is the case if the angle between the sun-earth line and the earth-probe line is greater than 16^o, which is true for the entire mission except 0.04 yr. on both sides of conjunction. The conclusion, then, is that filtering techniques which do not include the effects of the corona should be used until about 2 weeks before conjunction and should start again 2 weeks after conjunction. During the intervening 4 weeks, state estimation should be done through prediction, and data should be used to carry out the experiment.

2.4 Atmospheric and Ionospheric Effects

The atmosphere will refract electromagnetic radiation passing through it. It is assumed that a method exists of determining the azimuth and elevation angles of the incoming wave to within the stated accuracy regardless of refraction.

Electromagnetic radiation passing through the ionosphere will undergo a frequency shift. A method exists (4:104) for using two transmitted frequencies and their corresponding doppler shifts to eliminate first order effects of ionospheric frequency shift and reduce the higher order effects to the extent that they are on the order of 10^{-17} cps. Thus, this method can be used to reduce ionospheric frequency shift to a truly negligible level, so that this error source is not considered further.

2.5 Range-Rate Data and the Transmitter

Range-rate data will be available from the observed doppler frequency shift of the received signal. The governing equation (7:530) is

$$f_r = f_t \frac{1 - \dot{\rho}/c}{\sqrt{1 - (V/c)^2}} \tag{2.8}$$

where f_r is the received frequency, f_t is the transmitted frequency, $\dot{\rho}$ is the probe-earth range-rate and is positive for increasing range, and V is the total probe velocity. This can be rewritten as

$$\dot{\rho}/c = \frac{f_r - f_t}{f_t} + \frac{f_r}{f_t}\left(1 - \sqrt{1 - (V/c)^2}\right) \tag{2.9}$$

The first term represents the standard doppler effect. The second term represents a relativistic effect, the discussion of which is reserved for Chapter 5. In general, the maximum frequency shift due to range-rate is about 7.5 Kc/sec and the relativistic contribution is on the order of 1 cps.

The problem considered in this analysis is the estimation of probe state using the data available. The quality of the range-rate data depends upon a knowledge of the transmitted frequency. The transmitter now planned for use on board the Sunblazer probe is to broadcast at nominal frequencies of 75 Mc/sec and 225 Mc/sec. It has a long term stability of 1 part per 10^8 and a short term stability of 1 part per 10^7. The long term variations are somewhat difficult to describe. It seems likely, however, that over short periods of time (4 or 5 hours, for example) the long term frequency variations can be considered stationary at some value. The short term variations, then, are reasonably characterized as an additive, normally distributed noise having zero mean and a standard deviation of 7.5 cps. The correlation time of this noise is assumed to be small compared to any sampling period that might be used to receive data. Over longer periods of time, the mean value of the transmitted frequency will probably be subject to a time dependent drift and, additionally, may have a temperature dependent drift caused by changes in the distance of the probe from the sun. For the time being, the transmitted frequency, $f_t(t)$, will be written as

$$f_t(t) = f(t) + n(t) \tag{2.10a}$$

where

$$\overline{n(t)} = 0 \quad \text{and} \quad \overline{f_t(t)} = f(t) \tag{2.10b}$$

Here, $f(t)$ is the time dependent mean value. It is assumed that $f(t)$ is either known (deterministic) or can be estimated so well that it is deterministic compared to other frequency uncertainties in the system.

Because of the difficulty in describing the mean value of the transmitted frequency as a function of time, a different approach to the problem is taken. If it is assumed that transmitter drift is known and can be accounted for in the detected doppler shift, then the residual frequency uncertainties, due to short term transmitter variations and, perhaps, errors in detection, are assumed to cause the measured range-rate data to be a normally distributed random variable with a mean value equal to the true range-rate. The standard deviation of this distribution, $\sigma_{\dot{\rho}}$, is a measure of the quality of the range-rate data, and can be interpreted in terms of the residual frequency uncertainties. Range-rate data of varying quality is used to estimate probe state. A figure of merit (described in Chapter 4) then permits comparison of the uncertainties in the estimated probe state for various values of $\sigma_{\dot{\rho}}$. These results are then interpreted to specify the level of certainty required of the transmitted frequency in terms of which error sources must be considered (e.g., relativistic effects) and how well the long term frequency variations must be known to gain a given reduction in uncertainty of the estimate of probe state. This is discussed in greater detail in Chapter 5.

2.6 Circular Earth Orbit

If the earth is in an elliptic orbit, its position and velocity vectors are relatively complicated functions of time when they are written in a flight-path coordinate system centered at and defined by the probe. This particular coordinate system (described in Appendix B.2c) is to be used because in many respects it is the most convenient. The purpose of this analysis is to determine how well the probe state can be estimated using the available data. Because earth position and velocity are known well, the analysis here will not be appreciably effected by assuming a simpler model of the earth's orbit, as long as the model is a reasonable approximation to the true orbit. Hence, by assuming that the earth is in circular orbit, which is reasonable because its eccentricity is only 0.01673, we have the gain that earth position and velocity

in the probe centered coordinate system are simple sinusoidal functions of time from injection of the probe into elliptic orbit. A further gain is that the analysis can be carried out for an arbitrary launch date.

Another aspect of this assumption is that in reality it is the earth-moon barycenter that orbits the sun. The additional velocity of a point on the surface of the earth due to rotation about the barycenter is about 0.3×10^{-2} AU/yr. In terms of frequency shift, this motion can contribute as much as 4 or 5 cps to the apparent doppler shift due to range-rate. (A summary of comparative frequency shifts is given in Table 2.1) Because of the simplified model chosen for the earth's orbit, this effect is not considered. For state estimation of an actual probe, the analysis presented here would need to be modified by specifying a launch date and considering a more accurate earth orbit, which is elliptic motion of the barycenter around the sun, and motion of the earth about the barycenter.

A further aspect that needs to be considered is rotation of the earth about its axis. In this analysis, the difficulty has been circumvented by assuming that the data has been measured at an earth-centered receiving station. However, frequency shift due to the rotational velocity of the receiving station on the earth's surface can be on the order of 100 cps (maximum), so that earth rotation definitely must be considered in processing the real data.

2.7 The Nominal Probe Orbit

The probe is to be placed in a nominal orbit that has the following properties. Injection occurs at the time the probe crosses the earth's sphere of influence and at aphelion of the heliocentric, two-body ellipse. Aphelion radius is 1 AU and perihelion radius is 0.528 AU. The period is 2/3 yr, so that superior conjunction occurs 1 yr after injection and at perihelion of the probe orbit. The inclination of the nominal trajectory to the ecliptic plane is 0°. The probe will never actually follow this nominal trajectory. An actual trajectory that considers the gravitational attraction of bodies other than the sun can be calculated. However, this would seriously complicate the analysis presented here, and would seem to offer no particular benefit, because the assumed nominal is a good enough approximation to permit investigation of the state estimation problem without jeoperdizing the validity of the conclusions drawn (Chapter 5) from the investigation. For an actual

probe, however, the analysis provided here would need to be modified to include the true probe trajectory.

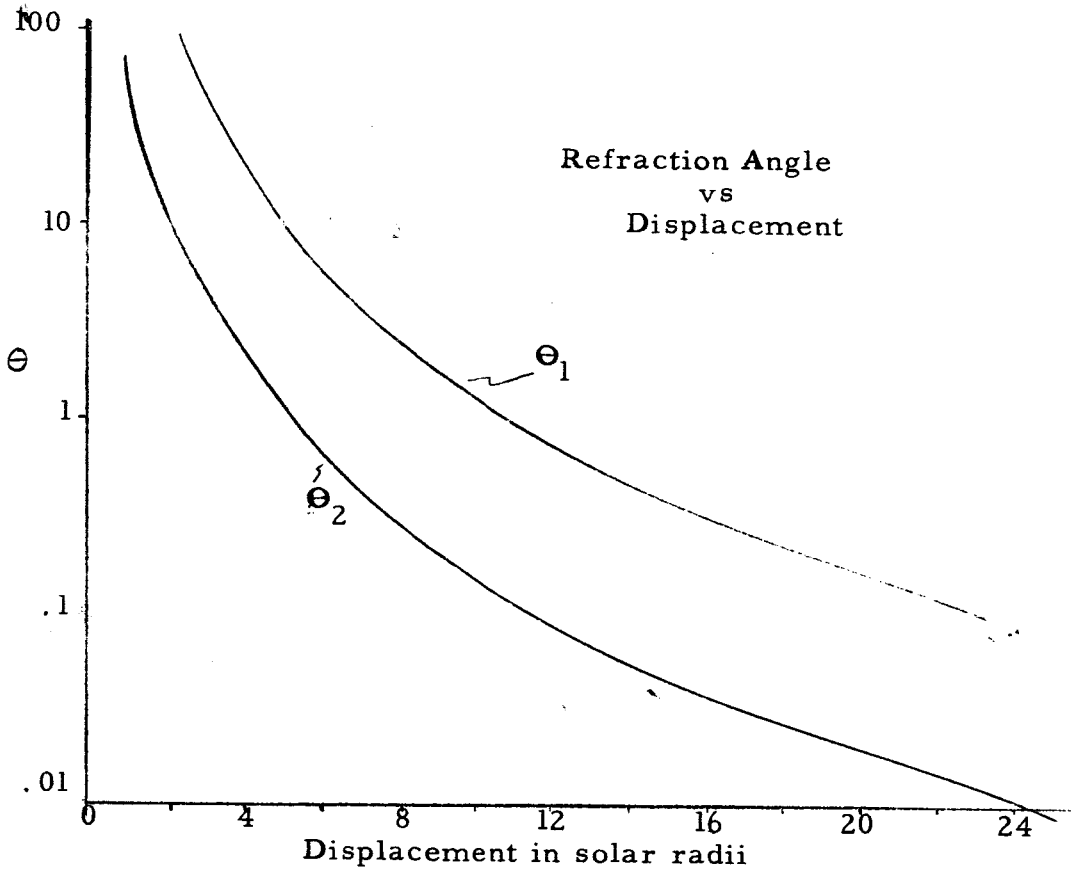

Figure 2.1 (Θ in minutes of arc)

Figure 2.2 ($\phi_{o,2}$ on top, right scales)

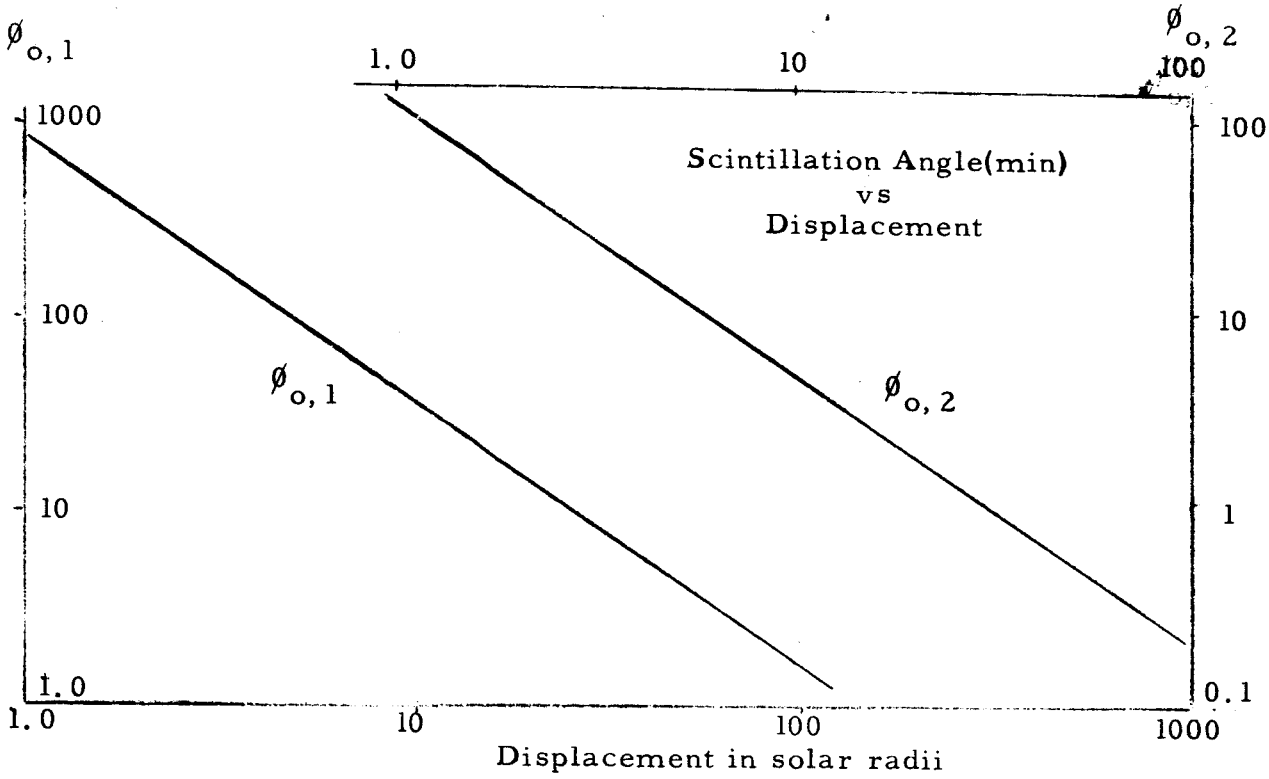

TABLE 2.1

RELATIVE SIZES OF FREQUENCY SHIFTS (75 Mc/sec Signal)

Cause	Approximate Frequency Shift
Range-rate	7.5 Kc/sec (maximum)
Relativistic effect	1 cps (order of magnitude)
Short-term transmitter uncertainty	7 1/2 cps (standard deviation)
Long-term transmitter uncertainty	Long-term drift assumed deterministic
Ionospheric Scattering	Unknown
Ionospheric Scattering, corrected using 2 frequency method	10^{-17} cps (Order of magnitude)
Rotation of earth about axis	100 cps (maximum)
Rotation of center of the earth around earth-moon barycenter	4 cps (maximum)

CHAPTER 3

MEASUREMENT VECTORS AND DEVIATIONS

In developing a method for determining Sunblazer position and velocity from measurements, it is useful to linearize the problem around a nominal trajectory and consider deviations away from this nominal. The development shows that deviations in the measurements are related to deviations from the nominal trajectory in position and velocity through functions called measurement vectors. These measurement vectors depend upon both time and the nominal trajectory. The derivation of the measurement vectors and their evaluation along the nominal trajectory are the subject of this chapter.

3.1 The State Deviation Vector and Measurement Deviations

The six components of Sunblazer position and velocity constitute a state vector, $\underline{x}(t)$. Based upon a precalculated (nominal) trajectory it is possible to calculate the values of measurable quantities as functions of time and nominal spacecraft state, $\underline{x}_N$. Due to unknown launch errors, and perturbing accelerations not considered in determining the nominal trajectory, the actual state will differ from the nominal state by the state deviation vector, $\delta\underline{x}$.

$$\delta\underline{x} = \underline{x} - \underline{x}_N \tag{3.1}$$

The state vector and most other variables used are functions of time. Because, in general, we are interested in them at some specific time, their functional dependence upon time will be suppressed until it is needed.

It is possible to write a very general relation for the measurable quantities as functions of nominal state.

$$m_N = f(\underline{x}_N) \tag{3.2}$$

Here, m_N is any measurable quantity, and $f(\underline{x}_N)$ is some corresponding scalar function. On the actual trajectory, the quantity we ought to measure can be written as

$$m = f(\underline{x}) \tag{3.3}$$

This differs from m_N because the actual state differs from the nominal state by $\delta\underline{x}$. The measurement deviation, δm, due to actual state deviation can be written as

$$\delta m = m - m_N \tag{3.4}$$

It would be expected that non-nominal perturbations and launch errors are small enough to keep $\delta\underline{x}$ small. If this is true we would hope to find that measurement deviations can be approximated as linear functions of the state deviation at any specified time.

If equation 3.3 is expanded in a Taylor Series expansion about the nominal state (See Appendix B.1), this in fact happens, and the result is

$$\delta m = \underline{h}^T \delta\underline{x} \tag{3.5}$$

The measurement vector, $\underline{h}$, is a function of time, and at any specified time is evaluated at the nominal state.

3.2 The Measurable Quantities

As now envisioned, the receiving station for the Sunblazer project will be located at El Campo, Texas. Using a phased array antenna, the azimuth and elevation angles of the received signal, and hence the spacecraft, with respect to an earth station can be determined within a certain accuracy. Furthermore, doppler data will be available, from which range-rate can be inferred, within certain bounds. The limitations on measurement accuracy are discussed at the end of Chapter 2.

For the purpose of this analysis, it is assumed that some technique exists for transforming this information to the center of the earth, where, at any specified time, we have three measurements. These are range-rate, elevation angle, and azimuth angle in some useful coordinate system. (Coordinate systems are discussed in Appendix B.2)

Because we cannot measure perfectly, the measurement deviation we actually measure, $\delta\tilde{m}$, differs from the deviation we ought to measure, δm, by an amount α. It is assumed that the three measurements have statistically independent and unbiased errors. Then,

$$\delta\tilde{m} = \delta m + \alpha \tag{3.6}$$

$$\text{and } \overline{\delta\tilde{m}} = \overline{\delta m} \tag{3.7}$$

It is also assumed that the measurement error, α, is independent of the true measurement deviation, δm; and that $\delta\tilde{m}$ is normally distributed about δm, the true measurement deviation. Then, $\overline{\alpha^2}$ is the variance of this normal distribution. These assumptions will be of use in the next chapter, which gives a procedure for state deviation estimation.

The measurable quantities are azimuth, A; elevation, L; and range-rate, $\dot{\rho}$. The azimuth and elevation angles are functions of position only. Consequently, we can write

$$\delta A = \underline{k}^T \delta\underline{x} = \left[\underline{k}_3^T \vdots \underline{0}_3^T\right] \underline{x} = \underline{k}_3^T \delta\underline{R} \tag{3.8a}$$

$$\delta L = \underline{d}^T \delta\underline{x} = \underline{d}_3^T \delta\underline{R} \tag{3.8b}$$

Range-rate deviation is a function of the entire state deviation, so that

$$\delta\dot{\rho} = \underline{c}^T \delta\underline{x} \tag{3.8c}$$

The vectors $\underline{k}$, $\underline{d}$, and $\underline{c}$ are the measurement vectors. For convenience in later use they are to be written in the flight-path coordinate system (described in Appendix B.2).

3.3 The Measurement Vectors in the Flight-Path Coordinate System

The measurement vectors are derived in an earth-centered (xyz) coordinate system in Appendix B, sections 3 and 5, and transformed into the flight-path coordinate system in Appendix B.4. The results are summarized below.

$$\underline{k}^T = \frac{1}{\rho}\left[\sin(A-\phi) \quad \cos(A-\phi) \quad 0 \vdots \underline{0}_3^T\right] \tag{3.9a}$$

$$\underline{d}^T = \left[0 \quad 0 \quad \frac{1}{\rho} \vdots \underline{0}_3^T\right] \tag{3.9b}$$

$$\underline{c} = \begin{bmatrix} \frac{1}{\rho^3}\left[(\underline{\rho}\cdot\underline{\rho})\,\dot{\underline{\rho}} - (\dot{\underline{\rho}}\cdot\underline{\rho})\,\underline{\rho}\right] \\ \hline \underline{\rho}/\rho \end{bmatrix} \tag{3.9c}$$

The angle, ϕ, is the angle from the sun-earth line to $\underline{\rho}$.

$$\phi(t) = \lambda(t) - 2\pi t \tag{B.12}$$

The angle, λ, is defined in Appendix B, section 4.

These vectors are evaluated along the nominal trajectory at specified times. The procedure for doing this is outlined in the remainder of this chapter.

3.4 Determination of the Measurement Vectors Along the Nominal

When we make a measurement, the one variable we know well is time. Because the measurement vectors and the nominal values of the measurable quantities are functions of the nominal orbit, we must know the nominal state and certain other parameters as functions of time. This section describes the determination of these at any time. For the work which follows, Figure 3.1 will be of use. The units to be used are the year and the astronaumical unit (92.9 million miles). The orbit is assumed to be the known, two-body ellipse that was specified in Chapter 2.

a) Nominal Satellite Radius (magnitude) and Velocity Vector

For an ellipse we have the relationship:

$$R_N = \frac{a(1-e^2)}{1+e\cos f} \tag{3.10}$$

where all orbital elements are for the nominal elliptic trajectory. Here, f is the true anomaly and can be found at any time by specifying the time and solving Kepler's problem. There are numerous techniques for solving Kepler's problem, so that this aspect is not considered further.

For the satellite, the magnitude of the velocity is:

$$V_N = \left[\mu_s\left(\frac{2}{R_N} - \frac{1}{a}\right)\right]^{1/2} \tag{3.11}$$

The direction of V_N specifies $\underline{1}_q$. Hence,

$$\underline{V}_N^T = [\ 0 \quad V_N \quad 0\ ]_{pqu} \tag{3.12}$$

b) Nominal Satellite Radius Vector and Flight-Path Angle

The radius vector, $\underline{R}$, is to be expressed in the flight-path coordinate system. From Figure 3.1, it can be seen that to determine $\underline{R}$ requires knowledge of ψ, the flight-path angle. Use of equations 3.10 and 3.11 and the definition of angular momentum supply us with knowledge of ψ.

$$\underline{H}_N = \underline{R}_N \times \underline{V}_N \tag{3.13a}$$

$$\left|\underline{H}_N\right| = R_N V_N \sin\psi \tag{3.13b}$$

$$H^2 = \mu a(1 - e^2) \tag{3.13c}$$

Substitution of equations 3.13b into 3.13c and simplification with equation 3.10 gives

$$\psi = \sin^{-1} \frac{1 + e\cos f}{\sqrt{1 + 2e\cos f + e^2}} \tag{3.14}$$

This relation gives an angle in the first quadrant. However, at certain points on the orbit, ψ may be in the second quadrant. This can be taken care of by noticing that the quadrant of ψ depends upon the quadrant of f. (See Figure 3.3) Specifically,

$$\psi = \begin{cases} \sin^{-1} \dfrac{1 + e\cos f}{\sqrt{1 + 2e\cos f + e^2}}, & 0 \leq f \leq \pi \\ \pi - \sin^{-1} \dfrac{1 + e\cos f}{\sqrt{1 + 2e\cos f + e^2}}, & \pi \leq f \leq 2\pi \end{cases} \tag{3.15}$$

Knowing ψ, it is a simple task to write $\underline{R}_N$.

$$\underline{R}_N^T = [\sin\psi \quad \cos\psi \quad 0\ ]\ R_N \tag{3.16}$$

c) Nominal Magnitude of Range

From Figure 3.1 and the law of cosines we have

$$\rho_N^2 = R_N^2 + r^2 - 2Rr\cos(f+180 - 2\pi t) \tag{3.17a}$$

which reduces to

$$\rho_N = \left[R_N^2 + 1 + 2R_N\cos(f - 2\pi t)\right]^{1/2} \tag{3.17b}$$

d) Nominal Azimuth Angle

Using the law of sines and Figure 3.1, we find that

$$\frac{\sin A}{R} = \frac{\sin(f + 180 - 2\pi t)}{\rho} = -\frac{\sin(f - 2\pi t)}{\rho} \tag{3.18a}$$

so that

$$A_N = \sin^{-1}\left[-\frac{R_N}{\rho_N}\sin(f - 2\pi t)\right] \tag{3.18b}$$

e) Nominal Earth Position and Velocity Vectors

In the inertial (X, Y, Z) reference system, the earth's position and velocity vectors are:

$$\underline{r}_{XYZ}^T = \left[\cos 2\pi t \quad \sin 2\pi t \quad 0\right] \tag{3.19a}$$

$$\underline{v}_{XYZ}^T = \left[-2\pi \sin 2\pi t \quad 2\pi \cos 2\pi t \quad 0\right] \tag{3.19b}$$

Using the matrix equation B.13 with ϕ replaced by λ gives the desired result in the flight-path coordinate system.

$$\underline{r}_{XYZ}^T\, M^T = \underline{r}_{pqu}^T = \left[\cos(\lambda - 2\pi t) \quad -\sin(\lambda - 2\pi t) \quad 0\right] \tag{3.20a}$$

$$\underline{v}_{XYZ}^T\, M^T = \underline{v}_{pqu}^T = \left[2\pi \sin(\lambda - 2\pi t) \quad 2\pi \cos(\lambda - 2\pi t) \quad 0\right] \tag{3.20b}$$

where:

$$\lambda = \psi + f + \pi/2 \tag{3.21}$$

f) Nominal Range and Range-Rate Vectors

Straightforward vector addition now gives the range and range-rate vectors.

$$\underline{\rho}_N = \underline{R}_N - \underline{r} \tag{3.22a}$$

$$\dot{\underline{\rho}}_N = \underline{V}_N - \underline{v} \tag{3.22b}$$

3.5 Results

In order to determine any nominal variable then, we start by specifying the time and solving Kepler's problem for the true anomaly. The next step is to solve the equations presented above in the order given. These results are then used to evaluate the measurement vectors; $\underline{k}$, $\underline{d}$, and $\underline{c}$. Furthermore, the information calculated here also defines the nominal probe state and nominal values for the measurable quantities. Hence, we need only the measured quantities to determine the actual measurement deviations. These measured deviations, together with the measurement vector, will later be used to estimate the state deviation vector.

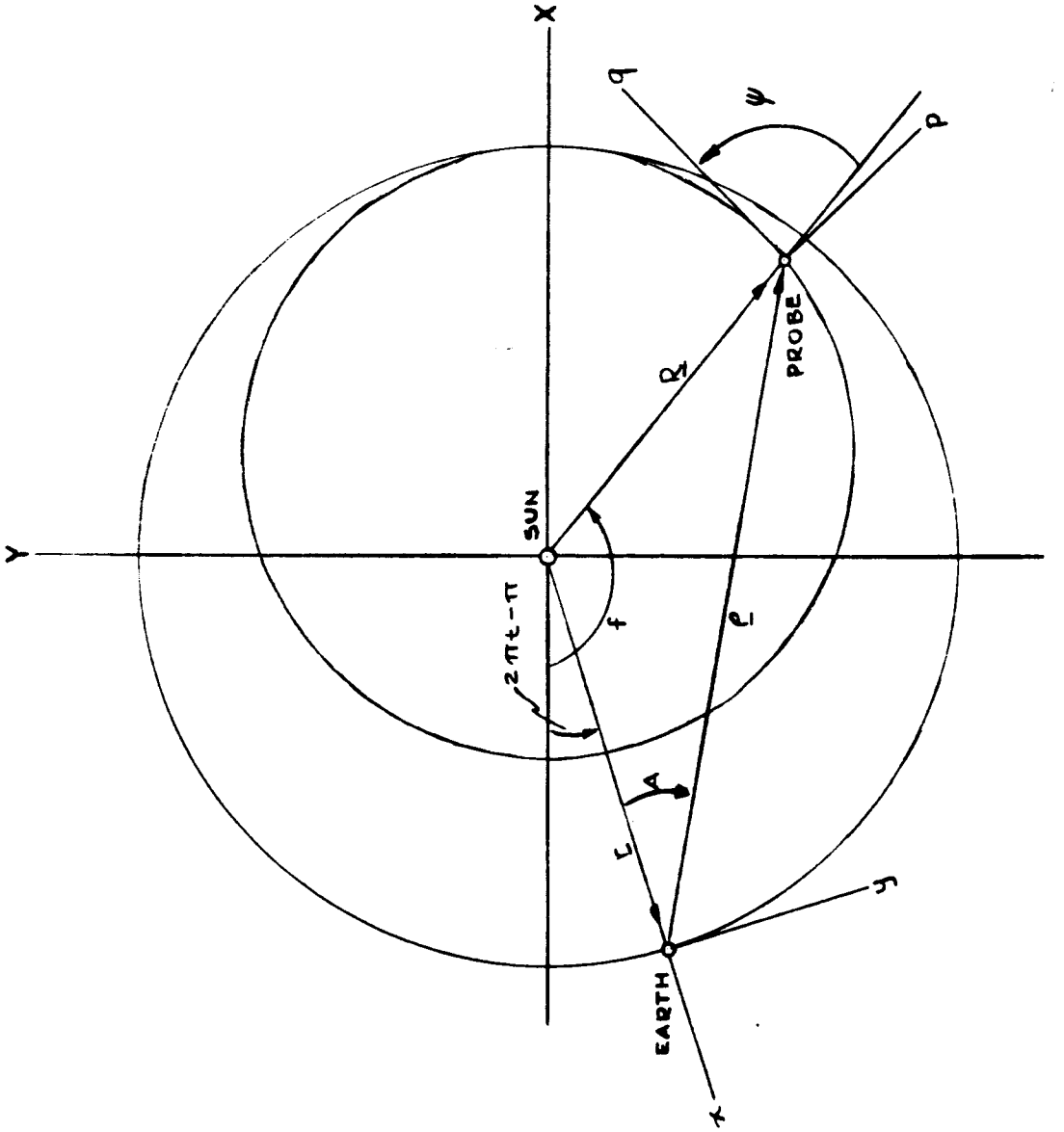

FIG. 3.1

CHAPTER 4

MAXIMUM LIKELIHOOD ESTIMATION AND THE FIGURE OF MERIT

As stated in the last chapter, the measurements actually made will yield measurement deviations which have errors. These measurement deviations are related to the state deviation at the measurement time, and the state deviation at any time can be extrapolated to any other time with the state transition matrix. Given enough measurements and the statistics of the measuring system, it is possible to estimate the state deviation. Two ways of doing this are discussed in this chapter. However, to estimate the state deviation, actual measurements are needed. On the other hand, the statistics of the measuring system are sufficient to determine how well the estimation procedure would work if "live" data were available. Consequently, the most important section of this chapter is that which develops a "figure of merit" for the estimation procedure. This figure of merit will give the level of uncertainty in the estimate that would be made if measurements were available.

4.1 The State Transition Matrix

The state transition matrix is a 6×6 matrix that relates the state deviations at different time points along the trajectory. A mathematical statement of this relation is:

$$\delta \underline{x}(t_n) = \Phi(t_n, t_{n-1})\ \delta \underline{x}(t_{n-1}) \tag{4.1a}$$

where Φ is the state transition matrix. For the remainder of this analysis, the notation will be shortened to

$$\delta \underline{x}_n = \Phi_{n,n-1}\ \ \delta \underline{x}_{n-1} \tag{4.1b}$$

Note also

$$\Phi_{n-1,n} = \Phi^{-1}_{n,n-1} \tag{4.1c}$$

If the nominal trajectory is an ellipse, the state transition matrix is an analytic function of the two time arguments. Writing the state deviation vector in a flight path coordinate system causes a further analytic simplification. (See Reference 12) This is the primary motive for assuming an elliptic nominal trajectory and writing vectors in the pqu frame.

In the following analysis the state transition matrix will be used to propagate the state deviation at one measurement time to other measurement times.

4.2 The Error Covariance Matrix

The estimate of the state deviation vector at time t_n is $\delta\hat{\underline{x}}_n$, and differs from the true state deviation by an error vector, $\underline{e}_n$.

$$\underline{e}_n = \delta\hat{\underline{x}}_n - \delta\underline{x}_n \tag{4.2}$$

The error covariance matrix, E_n, is defined as

$$E_n = \overline{\underline{e}_n \underline{e}_n^T} \tag{4.3}$$

The measuring system and the estimation procedure to be developed are such that each component of $\underline{e}_n$ is a normally distributed random variable, with zero mean, but not necessarily independent of the other components of $\underline{e}_n$. The diagonal elements of E_n are then the variances of the six components. This will be important later in the analysis. For now, the real importance of the error covariance matrix is that the sum of the diagonal elements (the trace) is a quadratic function of $\underline{e}_n$.

$$\mathrm{tr}[E_n] = \overline{e^2} = \overline{\underline{e}_n^T I \underline{e}_n} \tag{4.4}$$

4.3 Maximum Likelihood Estimation

It is assumed that, at any measurement time, the azimuth and elevation angles and range-rate are all measured. Then, after n measurement times, there are $3 \times n$ measurement deviations available that can be related to the state deviation at any point on the trajectory. These measurements can be "batch processed" to give a maximum likelihood estimate of the state deviation. (See References 2 and 11) It is shown in Reference 11 that any other method of filtering the

measurements in a manner that minimizes a quadratic function of $\underline{e}_n$ will yield an estimate that is identical to that obtained by "batch processing" the measurements. Consequently, a method of recursive estimation is developed below. This is a more convenient approach because "batch processing" can become cumbersome if the number of measurement times becomes large.

4.4 Recursive Estimation

Assume that, one way or another, there exists at time t_n a prior estimate of the state deviation vector, $\delta\underline{\hat{x}}_{n-1}$, and an associated error covariance matrix, E_{n-1}. Using the state transition matrix, these can be updated to time t_n.

$$\delta\underline{\hat{x}}'_n = \phi_{n,n-1} \quad \delta\underline{\hat{x}}_{n-1} \tag{4.5}$$

$$E'_n = \phi_{n,n-1} E_{n-1} \phi^T_{n,n-1} \tag{4.6}$$

At this point it is useful to define a measurement deviation vector, made up of the set of measured measurement deviations; $\delta\tilde{A}_n$, $\delta\tilde{L}_n$, and $\delta\tilde{\dot{\rho}}_n$.

$$\delta\underline{\tilde{m}}_n = \begin{bmatrix} \delta\tilde{A}_n \\ \delta\tilde{L}_n \\ \delta\tilde{\dot{\rho}}_n \end{bmatrix} \tag{4.7}$$

Specializing equation 3.6 to the measurements available gives

$$\delta\underline{\tilde{m}}_n = \begin{bmatrix} \delta A_n \\ \delta L_n \\ \delta \dot{\rho}_n \end{bmatrix} + \begin{bmatrix} \alpha \\ \beta \\ \gamma \end{bmatrix} = \delta\underline{m}_n + \underline{\mu}_n \tag{4.8}$$

Based upon the relations above, it is possible to formulate an estimation procedure that uses the prior estimate, updated with the transition matrix, and a weighted difference between the measured deviations and an estimate of what the deviations ought to be.

$$\delta\underline{\hat{x}}_n = \delta\underline{\hat{x}}'_n + W_n [\, \delta\underline{\tilde{m}}_n - \delta\,\underline{\tilde{m}}'_n] \tag{4.9}$$

where

$$\delta \underline{\tilde{m}}'_n = \begin{bmatrix} \underline{k}^T \\ \underline{d}^T \\ \underline{c}^T \end{bmatrix} \delta \underline{\hat{x}}'_n = H_n \quad \delta \underline{\hat{x}}'_n \tag{4.10}$$

W_n is the filter, and is to be chosen to minimize the trace of the error covariance matrix, which is a quadratic function of $\underline{e}_n$. This filter is derived in Appendix D using standard variational techniques, and is shown to satisfy both necessary and sufficient conditions. The result is an optimum filter, W_n^o, which gives a maximum likelihood estimate of the state deviation vector.

$$W_n^{oT} = [H_n E'_n H_n^T + A_n]^{-1} H_n E'_n \tag{4.11}$$

where A_n is the correlation matrix of measurement errors.

$$A_n = \overline{\underline{\mu}_n \underline{\mu}_n^T} = \begin{bmatrix} \overline{\alpha^2} & 0 & 0 \\ 0 & \overline{\beta^2} & 0 \\ 0 & 0 & \overline{\gamma^2} \end{bmatrix} \tag{4.12}$$

The measurement errors are assumed to be independent and unbiased. Using the optimum filter permits the following recurcive formulas to be written.

$$\delta \underline{\hat{x}}_n = [I - W_n^o H_n] \delta \underline{\hat{x}}'_n + W_n^o \delta \underline{\tilde{m}}_n \tag{4.13}$$

$$E_n = [I - W_n^o H_n] E'_n = E'_n [I - H_n^T W_n^{oT}] \tag{4.14}$$

Equation 4.13 permits maximum likelihood estimation of $\delta \underline{x}_n$ when real measurements are available. Equation 4.14, however, is a function only of the statistics of the measurement system, the measurement vectors, and some initial error covariance matrix. The diagonal elements of E_n give the variance of the estimation error in each of the six components of the state vector. Consequently, although the state deviation vector itself cannot be estimated, equation 4.14 permits determination of how good the estimate would be if live data were available. This is an important result, because if gives a relationship that can be used to determine the sensitivity of the estimation uncertainties

to uncertainties in the measurements available.

4.5 Figure of Merit

As outlined previously, the approach taken in this analysis was to assume that the measured data have certain statistical properties, and then interpret these properties in terms of the level of knowledge required of the transmitted frequency and the error sources. More specifically, angular measurements were assumed to be normally distributed with standard deviations of $1/10^{o}$. Range-rate data was also assumed to be normally distributed, but the standard deviation, $\sigma_{\dot{\rho}}$, was defined as a variable. This permits a comparison of the state estimate for range-rate data of varying quality. This standard deviation then becomes a measure of how well the transmitted frequency must be known, and what error sources must be considered, to estimate the probe state to a specified level of uncertainty.

To determine the sensitivity of the state estimate to the quality of range-rate data, a figure of merit was needed. An obvious choice was to use the diagonal terms of the error covariance matrix at some point on the trajectory. The point selected was superior conjunction, because it is during the time period just before and after conjunction that the primary Sunblazer experiment is to be carried out.

Equation 4.14 provides a method of calculating the error covariance matrix. However, because of the availability of a computer program, an alternate method was used to determine the error covariance matrix. The program is a modification of a program written by Mr. John Fagan of the Experimental Astronomy Laboratory, M.I.T. The modified program is included in Appendix A. The error covariance matrix is calculated in the following manner.

$$E_n^{-1} = E_n'^{-1} + H_n^T A_n^{-1} H_n \tag{4.15}$$

In Appendix D it is shown that, if the error covariance matrix is calculated by taking the inverse of equation 4.15, the result is identical to the error covariance matrix as calculated using equation 4.14. Taking t_n as the last measurement time before conjunction, and expanding $E_n'^{-1}$ in terms of an updated covariance matrix and measurements made at time t_{n-1}, we find that

$$E_n^{-1} = \phi_{n,n-1}^{T-1} E_{n-1}^{-1} \phi_{n,n-1}^{-1} + H_n^T A_n^{-1} H_n$$

$$= \phi_{n,n-1}^{T-1} [\phi_{n-1,n-2}^{T-1} E_{n-2}^{-1} \phi_{n-1,n-2}^{-1} + H_{n-1}^T A_{n-1}^{-1} H_{n-1}] \phi_{n-1,n-2}^{-1}$$

$$+ H_n^T A_n^{-1} H_n \tag{4.16}$$

If we continue to expand E_i^{-1} all the way back to injection (I) and simplify using

$$\phi_{n,t}^{T-1} = \phi_{n,n-1}^{T-1} \phi_{n-1,n-2}^{T-1} \cdots \phi_{t+1,t}^{T-1} \quad , \; n > t \geq I \tag{4.17}$$

the result is

$$E_n^{-1} = \phi_{n,I}^{T-1} E_I^{-1} \phi_{n,I}^{-1} + \sum_{i=0}^{N} \phi_{n,i}^{T-1} H_i^T A_i^{-1} H_i \phi_{n,i}^{-1} \tag{4.18}$$

This is then updated to conjuction. The error covariance matrix at conjunction is calculated using equation 4.19.

$$E_c^{-1} = \phi_{c,I}^{T-1} E_I^{-1} \phi_{c,I}^{-1} + \sum_{i=0}^{N} \phi_{c,i}^{T-1} H_i^T A_i^{-1} H_i \phi_{c,i}^{-1} \tag{4.19}$$

To use equation 4.19, the error covariance matrix at injection of the probe into its heliocentric elliptic orbit is needed.

4.6 The Covariance Matrix at Injection

Injection (subscript I) is defined as the time at which the probe crosses the earth's sphere of influence, and is assumed to occur at time zero and at aphelion on the nominal trajectory. It is assumed that at injection the best available extimate of the state deviation vector is zero (i.e., no measurements have been made).

With $\delta\underline{\hat{x}}_I = 0$, the actual probe state differs from the nominal state by exactly the negative of the error vector.

$$\delta\underline{\hat{x}}_I = -\underline{e}_I \tag{4.20}$$

The error covariance matrix at injection becomes

$$E_I = \overline{\delta\underline{x}_I \; \delta\underline{x}_I^T} \tag{4.21}$$

It is assumed here that burnout errors are independent and unbiased, and that they can be extrapolated along an escape hyperbola (with respect to the earth) to the sphere of influence, where they are still assumed to be independent (at injection only) and unbiased. This means that the elements of E_I will be zero everywhere except on the main diagonal. On the main diagonal, the elements will be the variances of the burnout errors, extrapolated to injection.

The evaluation of these variances is done in Appendix C. The variances are calculated for the following mission. (9:47)

launch date	22 July, 1966
payload	24 lbs.
launch azimuth	120^o
launch elevation angle	73.8^o
period	2/3 yr.
aphelion radius	1 AU
perihelion radius	.528 AU
inclination to the ecliptic	0^o
launch site	Wallops Island

This particular mission was selected because this is a typical mission for which data was available from a Ling-Temco-Vought, Inc., Astronautics Division feasibility study (Reference 9). Nineteen major error sources were used in the study. The results of the study were standard deviations of 0.00057 AU in aphelion radius, 0.44^o in inclination angle, and 110 ft/sec in burnout velocity at a nominal burnout altitude of about 10^6 ft. Based on the calculations of Appendix C, the diagonal terms of the error covariance matrix at injection are

$$\sigma^2_{Rp} = \sigma^2_{Rq} = \sigma^2_{Ru} = 10.7 \times 10^{-8} \text{ (AU)}^2 \tag{4.22}$$

$$\sigma^2_{Vp} = \sigma^2_{Vu} = 15.3 \times 10^{-4} \text{ (AU/yr)}^2 \tag{4.23a}$$

$$\sigma^2_{Vq} = 2.9 \times 10^{-4} \text{ (AU/yr)}^2 \tag{4.23b}$$

These variances were used as the diagonal elements of the error covariance matrix at injection, for use in equation 4.19. In the actual data processing problem, measurements would be available every day. It was decided, however, that 30 measurement times would be sufficient to give a good indication of the sensitivity of the estimation

uncertainties to data uncertainties without using an inordinate amount of computer time. The error covariance matrix at conjunction was then calculated using 30 measurement times chosen more or less uniformly from t = 0.05 yr to t = 0.96 yr, except that the times were more dense during periods of relatively high range-rate. The results of these calculations and their interpretation is covered in Chapter 5.

CHAPTER 5

CONCLUSIONS AND SUGGESTIONS

The figure of merit calculations were carried out for range-rate data with a standard deviation varying from 300m/sec to 0.03m/sec. In terms of uncertainty of the residual frequency deviations, this is a range of 75 cps to 3/400 cps for nominal 75 Mc/sec signal. The output of the calculation was the 6 x 6 error covariance matrix at conjunction, E_c. Because of the assumption of normally distributed and unbiased measurement errors and the use of maximum likelihood estimation, the estimation errors are also normally distributed and unbiased. Thus, each diagonal element of E_c is the variance of the normal distribution of the corresponding component of the state vector, and the square root of this variance is the standard deviation. The standard deviations of the estimation errors in probe position and velocity were calculated for each assumed range-rate standard deviation. These results are given in tabular form in Table 5.1 and in graphical form in Figures 1.1 and 1.2. It is found that the uncertainty in the out-of-plane components of the state vector (as measured by their standard deviation) is decoupled from the range-rate data. It is found that, for the Sunblazer probe considered here, there is a reasonable expectation of reducing the uncertainties in the in-plane components by 80% compared to the uncertainty in the estimate if only angular data are filtered. This requires that the residual uncertainty of frequency deviations be reduced to 3/4 cps (standard deviation). Methods of achieving this are discussed in this chapter. It is also found that the estimation uncertainties can be reduced even more if a better frequency standard is available. This is also discussed, as are possible extensions of this analysis.

5.1 Out-of-Plane Components

Because the nominal trajectory used in this analysis lies in the ecliptic plane, the estimation uncertainties in the out-of-plane position and velocity are insensitive to frequency uncertainties. Because the azimuth angle, as measured from the hypothetical earth-centered receiving station, is measured in the ecliptic plane (see Figure B.1) my opinion is that the out-of-plane components are also insensitive to errors in the azimuth measurements. It was found that, for these components, the standard deviation in the position estimate, σ_{Ru}, is 4000 km and the standard deviation in velocity is 1.25×10^{-2} km/sec. These values arise when the standard deviation of the elevation angle errors is $1/10^{o}$. As a matter of interest, it was also found that if the standard deviation of the elevation angle errors was 1^{o}, then these uncertainties grow to 21,000 km and 1 km/sec respectively.

5.2 In-Plane Components

If only angular data are filtered, the uncertainties in the estimate of the in-plane components of position and velocity are

$$\sigma_{Rp} = 11{,}520 \qquad \sigma_{Rq} = 49{,}400 \text{ km} \tag{5.1}$$

$$\sigma_{Vp} = 1.98 \times 10^{-2} \text{ km/sec} \qquad \sigma_{Vq} = 4.73 \times 10^{-3} \text{ km/sec} \tag{5.2}$$

If range-rate measurements are incorporated into the estimation procedure, the uncertainties become functions of the quality of these measurements. (See Figures 1.1 and 1.2) The results of the calculations made for this analysis are given in tabular form in Table 5.1. This information indicates that if the residual uncertainty of the frequency deviations can be reduced to 3/4 cps, then the in-plane uncertainties can be reduced to less than 20% of the uncertainties given in equations 5.1 and 5.2 for the filtering of angular measurements only. These uncertainties are

$$\sigma_{Rp} = 2{,}220 \text{ km} \qquad \sigma_{Rq} = 7{,}420 \text{ km} \tag{5.3}$$

$$\sigma_{Vp} = 3.08 \times 10^{-3} \text{ km/sec} \qquad \sigma_{Vq} = 0.885 \times 10^{-3} \text{ km/sec} \tag{5.4}$$

It is interesting to compare these results to the results obtained by making a single measurement of the azimuth and elevation angles

just prior to conjunction. In this case, we can make no estimate at all of the probe velocity or its radial position. The two components that can be estimated are the tangential ($\underline{1}_p$) and out-of-plane ($\underline{1}_u$) position components, and the uncertainty of each of these is 386,000 km.

At levels of frequency uncertainty below 3/4 cps, it is found that for every order of magnitude the frequency uncertainty is reduced, the uncertainty in the estimate of the in-plane components is also reduced by about an order of magnitude. If more stable on board frequency standards become available in the future, then it would seem plausible to reduce the estimate uncertainty by appreciably more than 80%. However, for the transmitter now planned for use aboard the first Sunblazer probe, I feel that it is reasonable to assume that the incoming signal can be filtered sufficiently well to reduce the residual frequency uncertainty to the vicinity of 3/4 cps. (This filtering is distinct from the filtering of measurements with W_n^o to obtain the state deviation estimate, and is described in the next section.) To filter the incoming signal more in order to reduce the residual frequency uncertainty to a lower level may be somewhat unrealistic because of a lack of a truly deterministic function for the time dependent mean frequency, f(t). In the present context, it is assumed that if f(t) is not known, it can be estimated well enough that the uncertainty in f(t) is small compared to 3/4cps, so that for practical purposes, the estimate of f(t) may be considered deterministic. Suggestions for estimating f(t) are made in a later section.

5.3 Reduction of Residual Frequency Uncertainty

As stated previously, the transmitter can be characterized a having short-term frequency variations that are normally distributed about a known (or well estimated), time dependent mean frequency. The standard deviation of this distribution is 7.5 cps. The transmitter broadcasts for 100 msec once every 10 sec. The frequency that arrives at the receiving station will be the actual transmitted frequency reduced (or increased) by an amount that depends upon the actual range-rate and by a relativistic frequency shift. It is obvious that to reduce the residual frequency uncertainty to 3/4 cps, it will be necessary to correct the received data for this relativistic effect, as it constitutes a bias which is too big to be neglected. However, the compensation of this bias presents no real problem. The relativistic effect is small,

and based upon a present estimate of probe velocity it can be removed accurately enough that the error made in compensating it will be many orders of magnitude lower than the effect itself. Since the relativistic frequency shift is on the order of 1 cps, any error made in compensation due to an error in estimated probe velocity will be negligible. Because this effect can be removed, essentially without error, the remainder of this analysis assumes that this has been done during detection of the received frequency.

Detection of the received frequency may introduce an error in the measured doppler frequency shift. Additionally, other sources of frequency shifts, such as ionospheric scattering, may introduce errors. It is assumed here that if any of these other sources of frequency shift introduce a biased shift, then that bias will be removed as well as possible. The remaining frequency uncertainties are then lumped into what is assumed to be an unbiased, normal distribution, called the detection error, d(t), which has an unknown standard deviation. The analysis that follows will put a bound on that standard deviation. The detection errors are also assumed to have a correlation time small compared to 10 sec.

The doppler shift will be determined by comparing the detected frequency with a reference frequency which is the expected transmitter frequency, f(t). The errors at this point will be due to the detection errors, d(t), and the transmitter variations, n(t). The problem then becomes one of filtering this measured doppler shift in such a way that the residual frequency uncertainty due to d(t) and n(t) is on the order of 3/4 cps. The following solution is recommended.

The detected frequency shift is a random process which has stationary statistics, but it involves a frequency shift due to range-rate that is time varying. However, over short periods of time (an hour), the range-rate varies so little that the process can be considered time invariant. Then, with the doppler shift samples we measure on the ground every 10 sec, it is possible to estimate the mean doppler shift by taking an average of a finite number of individual doppler shift samples. This average value is the number chosen for the doppler shift and is itself a random variable with a normal distribution that can be calculated from the statistics of the measured doppler shift samples.

The receiving station normally can receive data for 2 to 3 hours daily. It is suggested that samples of the doppler shift be taken every 10 sec for 67 min, for a total of 400 samples. The estimate of the true doppler shift, $M_{\Delta f}$, becomes

$$M_{\Delta f} = \frac{1}{400} \sum_{i=1}^{400} \Delta f_i \tag{5.5}$$

where Δf_i is a single sample. Note that $M_{\Delta f}$ is an unbiased estimator, so that the mean value of $M_{\Delta f}$ is the true doppler shift, Δf.

$$\overline{M_f} = \frac{1}{400} \sum_{i=1}^{400} \overline{\Delta f} + \overline{n(ti)} + \overline{d(ti)} = \Delta f \tag{5.6}$$

As stated above, the standard deviation of $M_{\Delta f}$, σ_M, can be calculated from the statistics of n(t) and d(t). The standard deviation of d(t) is unknown. Furthermore, we have already specified the desired level of residual frequency uncertainty as 3/4 cps. Having specified this, and knowing the standard deviation of n(t), σ_n, it is now possible to put a bound on the standard deviation of d(t).

$$\sigma_M^2 = \frac{\sigma_n^2 + \sigma_d^2}{400} \tag{5.7a}$$

$$\sigma_d \approx 15 \text{ cps} \tag{5.7b}$$

It is unlikely that the detection errors will have a standard deviation approaching 15 cps for the following reasons. Frequency shift due to Brillouin scattering will not contribute an appreciable error because prediction will be used to estimate probe state during that time period when it could be a factor. Ionospheric frequency shift can be reduced to the order of 10^{-17} cps. Errors caused by the ground equipment used to determine the doppler shift samples ought to be negligible because this equipment is maintained in a laboratory environment where size and weight are not a factor. Therefore, the frequency stability of this equipment ought to be several orders of magnitude better than the equipment in the spacecraft, and the frequency errors should be no larger than a few parts in 10^{11} or 10^{12} (on the order of 0.001 cps or smaller). Assuming detection errors are totally negligible, it is possible to say that the standard deviation of the measured Δf will be 3/8 cps, which permits reduction in the estimation uncertainties to

about 10% of the values calculated when only angular data is filtered.

In the actual processing of data, it is probably more convenient to determine doppler shift samples with a precision frequency standard as the reference to be compared with the detected frequency. This frequency standard would be set at the initial frequency of the onboard transmitter and left unchanged. The doppler shift samples would be processed as above to obtain an uncompensated average shift, $M'_{\Delta f}$. Relativistic effects, onboard transmitter drift, and biases, would be calculated and stored in the data processing computer. They would be used after calculation of $M'_{\Delta f}$ to correct $M'_{\Delta f}$ to give $M_{\Delta f}$. This method of processing the data is shown in block diagram form in Figure 5.1.

5.4 Suggestions for the Determination of f(t)

The analysis presented above assumes that the time dependent mean frequency of the transmitter, f(t), is either deterministic or can be well estimated. It is highly unlikely that f(t) will be a deterministic function of time. Some suggestions are offered here for estimating it.

The analysis here assumed measurements were made at 30 points during the mission between injection and conjunction. In fact, data will be available for state estimation daily for about 350 days prior to conjunction, and for a considerable time after conjunction. The following method is proposed as a possible way of determining f(t). At time t=0 (injection), the transmitted frequency should be very close to the nominal value of 75 Mc/sec. Measurements should be made and used with the filter W_n^o to make a state estimate.

$$\underline{x}_1 = \underline{x}_{N,1} + \delta\underline{x}_1 \tag{5.8}$$

where $\underline{x}_{N,1}$ is the nominal state at time t_1. Until the next time a state estimation (through filtering) is desired, the initial estimate should be updated daily with the state transition matrix and an estimate of range-rate should be made based upon $\underline{x}_1$. This figure should then be compared to the apparent range-rate based upon $M_{\Delta f}$ and f(t) = 75 Mc/sec. This will produce an apparent error in the range-rate. If it is then assumed that, for the period between filtered state estimates,

$$f(t) = (1 + a\,t) \times 75\,\text{Mc/sec} \tag{5.9}$$

a value of "a" can be selected that will minimize the mean squared error in apparent range-rate. For the next interval between filtered state estimates, f(t) is assumed to be given by equation 5.9. Again, there will be apparent range-rate errors, so that a new estimate of "a" will be made. This process would be continued for the entire mission until prediction begins (t = 0.96 yr), and would be resumed again after prediction ends (t = 1.04 yr). This approach is offered as a solution that might estimate f(t) well enough. How well this method will estimate long-term drift was not investigated.

An alternate approach, and probably a superior one, is to hypothesize a model for the transmitter. A possibility is

$$f(t) = f_N(1 + a\,t) \tag{5.10}$$

where f_N is 75 Mc/sec, and "a" is the oscillator drift rate. The problem now would be reformulated and "a" would be added to the state deviation vector and this parameter would be estimated along with the position and velocity deviations. This would require derivation of a new measurement vector for range-rate and would result in a different optimum filter. Measurements could then be made daily for the purpose of state estimation.

These methods were not analyzed in depth and are suggested as possible areas in which this analysis could be extended. A final possibility is that frequency standards of better quality may become available for this type of application. For example, a Rubidium gas cell controlled oscillator with a short term stability of 1 part per 10^{11} and a long term drift of less than 3 parts per 10^{11} per month is commercially available. The device weighs 24 pounds and has a frequency of about 6800 Mc/sec. (Reference 13) This frequency could be counted down to a level useful for the Sunblazer experiment, probably without seriously affecting the long and short term stability of the overall system. If this frequency standard were somewhat lighter or if some future mission uses a larger probe, then this type of device would probably permit transmitter drift to be totally neglected without effecting our ability to reduce the residual frequency uncertainties to 3/4 cps. However, with a standard this good, it would seem more beneficial to

estimate the drift and to filter out the short term variations, as this would decrease the uncertainties in the estimated state by 1 or 2 orders of magnitude.

5.5 Modifications for a Real Mission

As mentioned previously, several simplifying assumptions were made that prevent this analysis from being directly applicable to a real mission. The modifications required to use the data processing procedures set forth here are given in this section.

The analysis must be formulated for a receiving station on the earth's surface. It is possible to transform the azimuth and elevation angles to the center of the earth. The same is not true for range-rate data because there is no measurement of the probe velocity component in the plane perpendicular to the probe-ground station line. I believe, however, that it may be possible to achieve a very good, approximate transformation using measured range-rate and an estimate based on the present estimated state, of the velocity in the plane perpendicular to the probe-ground station line. I feel this possibility ought to be investigated, as this may result in a more manageable mathematical description than found by formulating the analysis in ground station coordinates.

The effects of the rotation of the earth about the earth-moon barycenter must be taken into consideration. Also, the ellipticity of the orbit of the barycenter must be accounted for.

The effect on the probe of gravitating bodies other than the sun will probably produce a trajectory that differs from the assumed nominal ellipse by enough to cause large state deviations. If these deviations become too large, then the assumption that measurement deviations are linearly related to state deviations (equation 3.5) will not be true. There are two possible solutions to this difficulty. The first is to rectify the nominal ellipse (described below) to an ellipse that more closely approximates the actual trajectory. The other solution is to integrate the many-body equations of motion to get a more accurate (and non-conic) nominal trajectory. This approach also requires that the state transition matrix be calculated by numerical integration.

5.6 The Transponder and Rectification of the Nominal Orbit

As mentioned previously, the probe contains a beacon-transponder that will operate for about a week. This device permits determination of range and range-rate data as well as the azimuth and elevation angles.

Consequently, there is no real need to extrapolate burnout errors to injection to get the error covariance matrix at that point. Likewise, there is no need to assume that the nominal trajectory is the one we really desired (2/3 yr period and in the ecliptic). I suggest that a filter be developed that estimates the state deviation vector from the time of burnout to injection. At injection, this estimate, $\delta\hat{\underline{x}}_I$, is used to define a new nominal trajectory on which the estimated state deviation is zero. Furthermore, by filtering between burnout and injection, the error covariance matrix can be determined recursively from burnout, and will be available at injection for use in the filtering procedure developed in this analysis.

The concept of defining a new nominal by finding the trajectory that makes the estimate of the state deviation zero is known as rectification. The use of rectification is not limited to injection. Any time the state deviation vector gets large enough to endanger the validity of the assumption (equation 3.5) that the measurement deviations are linearly related to state deviations, then the nominal orbit ought to be rectified. This causes the state deviation vector to be zero. The process leaves the error covariance matrix unchanged, with the exception that it may need to be rotated into a more convenient coordinate system. It also requires that new relations be used for evaluating the measurement vectors along the nominal. The question of how large state deviations may grow before equation 3.5 loses its validity is left unanswered and is suggested as an area in which this study might be extended.

5.7 Prediction and Smoothing

The primary Sunblazer experiment will take place during a time period of about 2 weeks on both sides of conjunction. During this 4 week interval, received data will be corrupted with errors which are poorly known. Consequently, it has been suggested that probe state be estimated by prediction rather than filtering during this period. If the filtered estimate of the state deviation vector made at the last measurement time before conjunction (t = 0.96 yr) is $\delta\hat{\underline{x}}_F$, then the predicted state deviation is

$$\delta\hat{\underline{x}}_t = \underline{\Phi}_{t,F}\ \delta\hat{\underline{x}}_F \tag{5.11}$$

where t is any time during the 4 weeks around conjunction.

After the experiment has been performed ($t \geq 1.04$ yr), data will again be available for estimating the state deviation through filtering. This means that data will be available on both sides of the conjunction interval, and interpolation can be used to achieve a better estimate of the state deviation during the time of the experiment than the estimate available through prediction alone. This process, known as smoothing, is not investigated in this study. I suggest that the application of smoothing to the probe considered here might be a useful extension of this analysis.

TABLE 5.1

Position and Velocity Uncertainties for Selected Range-Rate Standard Deviations

$\sigma_{\dot{\rho}}$ m/sec	Equivalent σ_f cps	σ_{Rp} AU km	σ_{Rq} AU km	σ_{Vp} AU/yr km/sec	σ_{Vq} AU/yr km/sec	σ_{Ru} AU km	σ_{Vu} AU/yr km/sec
*		$.768 \times 10^{-4}$ 1.152×10^{4}	$.329 \times 10^{-3}$ 4.94×10^{4}	$.415 \times 10^{-2}$ 1.975×10^{-2}	$.994 \times 10^{-3}$ $.473 \times 10^{-2}$	$.265 \times 10^{-4}$ $.398 \times 10^{4}$	$.263 \times 10^{-2}$ 1.25×10^{-2}
300	75	$.768 \times 10^{-4}$ 1.151×10^{4}	$.328 \times 10^{-3}$ $.429 \times 10^{5}$	$.414 \times 10^{-2}$ 1.97×10^{-2}	$.992 \times 10^{-3}$ 4.72×10^{-3}	same	same
200	50	$.766 \times 10^{-4}$ 1.15×10^{4}	$.327 \times 10^{-3}$ $.49 \times 10^{5}$	$.413 \times 10^{-2}$ 1.965×10^{-2}	$.99 \times 10^{-3}$ 4.7×10^{-3}	same	same
100	25	$.759 \times 10^{-4}$ 1.14×10^{4}	$.323 \times 10^{-3}$ $.485 \times 10^{5}$	$.407 \times 10^{-2}$ 1.93×10^{-2}	$.982 \times 10^{-3}$ 4.67×10^{-3}	same	same
60	15	$.744 \times 10^{-4}$ 1.117×10^{4}	$.313 \times 10^{-3}$ $.47 \times 10^{5}$	$.395 \times 10^{-2}$ 1.88×10^{-2}	$.961 \times 10^{-3}$ 4.57×10^{-3}	same	same
30	7-1/2	$.682 \times 10^{-4}$ 1.02×10^{4}	$.275 \times 10^{-3}$ $.412 \times 10^{5}$	$.347 \times 10^{-2}$ 1.65×10^{-2}	$.882 \times 10^{-3}$ 4.2×10^{-3}	same	same
10	2-1/2	$.418 \times 10^{-4}$ $.625 \times 10^{4}$	$.149 \times 10^{-3}$ $.224 \times 10^{5}$	$.191 \times 10^{-2}$ 0.87×10^{-2}	$.543 \times 10^{-3}$ 2.58×10^{-3}	same	same
3	3/4	$.148 \times 10^{-4}$ $.222 \times 10^{4}$	$.495 \times 10^{-4}$ $.742 \times 10^{4}$	$.648 \times 10^{-3}$ 3.08×10^{-3}	$.194 \times 10^{-3}$ $.885 \times 10^{-3}$	same	same
.6	3/20	$.304 \times 10^{-5}$ $.456 \times 10^{3}$	$.1015 \times 10^{-4}$ $.151 \times 10^{4}$	$.1319 \times 10^{-3}$ $.61 \times 10^{-3}$	$.398 \times 10^{-4}$ 1.89×10^{-4}	same	same

TABLE 5.1 (continued)

	$\sigma_{\dot{\rho}}$	σ_f	σ_{Rp}	σ_{Rq}	σ_{Vp}	σ_{Vq}	σ_{Ru}	σ_{Vu}
	0.3	3/40	$.152 \times 10^{-5}$ $.228 \times 10^{-3}$	$.507 \times 10^{-5}$ $.76 \times 10^{-3}$	$.659 \times 10^{-4}$ 3.14×10^{-4}	$.199 \times 10^{-4}$ $.91 \times 10^{-4}$	same	same
	.06	3/200	$.305 \times 10^{-6}$ $.457 \times 10^{-2}$	$.101 \times 10^{-5}$ $.152 \times 10^{-3}$	$.132 \times 10^{-4}$ $.062 \times 10^{-4}$	$.399 \times 10^{-5}$ 1.9×10^{-5}	same	same
	.03	3/400	$.152 \times 10^{-6}$ $.228 \times 10^{-2}$	$.507 \times 10^{-6}$ $.76 \times 10^{-2}$	$.659 \times 10^{-5}$ 3.14×10^{-5}	$.199 \times 10^{-5}$ $.91 \times 10^{-5}$	same	same
**	.6	3/20	$.3045 \times 10^{-5}$ $.457 \times 10^{-3}$	$.1016 \times 10^{-4}$ $.152 \times 10^{-4}$	$.132 \times 10^{-3}$ $.62 \times 10^{-3}$	$.399 \times 10^{-4}$ 1.9×10^{-4}	$.1403 \times 10^{-3}$ $.21 \times 10^{-5}$	$.2 \times 10^{-1}$ .95

* On this computer run, no range-rate data was used.

** On this run, the standard deviations of the angular data were deteriorated to 1°. This result is included as a matter of interest.

Figure 5.1

The Range-Rate Measurement (75 Mc/sec signal)

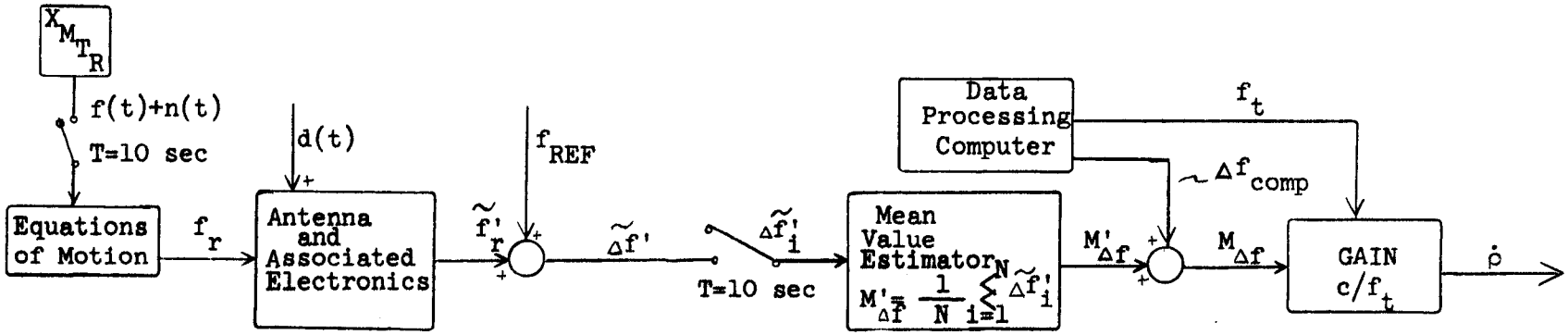

Explanation of Quantities

f(t)	mean value of transmitted signal
n(t)	short term transmitter noise
f_r	signal arriving at receiving station
d(t)	lumped detection errors
$\tilde{f}'_r$	measured, uncompensated, received frequency
f_{REF}	75 Mc/sec
T	sampling period
$\tilde{\Delta f}'$	measured, uncompensated, doppler shift
$\tilde{\Delta f}'_i$	i^{th} sample of $\tilde{\Delta f}'$
$M'_{\Delta f}$	uncompensated estimator of doppler shift
Δf_{comp}	compensation for relativity, long term transmitter drift, etc.
$M_{\Delta f}$	estimator of doppler shift due to range-rate
f_t	75 Mc/sec + drift
c	the speed of light

The recommended value for the number of samples, N, is 400.

APPENDIX A

THE COMPUTER PROGRAM

A.1 Description

The program consists of a main program and 14 subroutines, and is written in Fortran IV for use on an IBM System 360.

The main program is used for input/output and calls the subroutines that actually calculate the error covariance matrix at conjunction through use of equation 4.19. The inputs for the main program are the measurement times, ST(I); the measurement variances, SS(J); and the six non-zero diagonal elements of the initial error covariance matrix, EO(K,K). It calculates the sun's gravitational constant, U; the semi-major axis of the nominal trajectory, AM; the eccentricity of the nominal trajectory, E; and the mean angular motion AVN. The main program specifies the eccentric anomaly of the initial point on the trajectory, AI. The eccentric anomaly of the final point, EAP, is zero unless otherwise specified. (Here it is not specified, since conjunction occurs at perihelion.) The program then calls SUBROUTINE XTRP. XTRP extrapolates the initial covariance matrix to conjunction and inverts it. The program calls SUBROUTINE PERI, which adds in the effect of the measurements.

PERI is basically a loop that operates 30 times, once for each measurement time. PERI's first action it to call CCOM, which calls TRUE. TRUE has inputs of the eccentricity, E, and mean anomaly, A, and solves Kepler's problem for the eccentric anomaly, which is placed in common storage. CCOM also makes available the state transition matrix. PERI then calls VCTR three times. Each time it is called, VCTR calculates the 6 components of one of the measurement vectors and returns the result to PERI. PERI then incorporates the corresponding contribution of that measurement (a 6×6 matrix),

extrapolates it to conjunction, and uses **SUM** to add it to the 6 x 6 matrix of previous results and calls the result **EPI**. After all 90 measurements have been incorporated, **PERI** calls NVRT. NVRT inverts the 6 x 6 matrix **EPI** to give the error covariance matrix at conjunction, **EP**. This is returned to the main program, where it is printed. The main program then reads any new measurement variances and operates again, until no more data is supplied. It is also possible, by specifying N=2 in the main program, to avoid the use of range-rate data completely.

Subroutines **MTRM**, **MTRN**, **MTRS**, and **MTRT** are used to calculate the elements of the state transition matrix. **MPY1** multiplies a vector times its transpose. This is needed because of the manner in which the program includes the contribution of the measurements. Note that

$$H_n^T A_n^{-1} H_n = \frac{\underline{k}\ \underline{k}^T}{\alpha^2} + \frac{\underline{d}\ \underline{d}^T}{\beta^2} + \frac{\underline{c}\ \underline{c}^T}{\gamma^2} \qquad (A.1)$$

The program calculates the contribution of one measurement at a time, and **MPY1** calculates, for example, the 6 x 6 matrix $\underline{k}\ \underline{k}^T$. The division of $\underline{k}\ \underline{k}^T$ by the measurement variance, α^2 = SS(1), occurs in **PERI**. **MPY2** and **MPY3** give the products of matrices. Some of the programs operate in double precision. This is clearly indicated in the listing that follows by a **DOUBLE PRECISION** card.

Of the subroutines described above, VCTR was written entirely, and **PERI** was written in part, by the author. The main program was also written by the author. All other subroutines are modifications of the program described in Reference 6; both the original program and the modified subroutines are due to Mr. John Fagan. (See Reference 6)

A.2 Program Listing

The program listing is included in this section as a matter of record and begins on the next page.

```
/JOB      GO                          FAGAN
      COMMON EX(6,6),SS(3),ST(30),E,AVN,EAP,F,PI,U,AM
      DIMENSION CI(6,6),CIT(6,6),EPI(6,6),H(6),HH(6,6),S(6,6),
     1B(6,6),TM(3,3),TN(3,3),TS(3,3),TT(3,3),EP(6,6),EO(6,6)
     2,AA(6,6)
   94 FORMAT (3E30.10)
   93 FORMAT (6F18.9)
   44 FORMAT )///*
   91 FORMAT (6F6.3)
   92 FORMAT (3E15.10)
      READ (5,91) (ST(I), I=1,30)
      READ (5,92) (EO(K,K), K=1,6)
      WRITE (6,91) (ST(I), I=1,30)
      WRITE )6,44*
      N=3
   54 CONTINUE
      READ (5,92) (SS(J), J=1,3)
      PI=3.141593
      U=4639.7*(3.6*2.4*3.6525)**2/(9.29*5.28)**3
      AM=(4./9.)**(1./3.)
      E=1./AM-1.
      AVN=3.*PI
      AI=-PI
      WRITE (6,93) PI,U,AM,E,AVN,AI
      WRITE )6,44*
      WRITE (6,94) (SS(J), J=1,3)
      WRITE )6,44*
      WRITE (6,93) (EO(K,K), K=1,6)
      WRITE )6,44*
   53 CALL TRUE (E,AI,F,EAC)
      CALL XTRP (EO,EAC)
      CALL NVRT )AA,FX*
      WRITE (6,93) ((AA(I,J), I=1,6),J=1,6)
      WRITE )6,44*
      CALL PERI (N,EP)
      WRITE (6,93) ((EP(K,L), K=1,6), L=1,6)
      WRITE )6,44*
      IF (N-2) 51,51,52
   51 N=3
   52 CONTINUE
      GO TO 54
      END
/FTC     DECK
      SUBROUTINE VCTR (K,I,H)
      COMMON EX(6,6),SS(3),ST(30),E,AVN,EAP,F,PI,U,AM
      DIMENSION H(6)
      T=ST(K)
      IF (I-1) 5,6,5
    6 CONTINUE
      R=AM*(1.0-E**2)/(1.0+E*COS(F))
      V=SQRT(U*(2.0/R-1.0/AM))
      ROSQ=R**2+1.0+2.0*R*COS(F-2.0*PI*T)
      RO=SQRT(ROSQ)
      COSA=(1.0+ROSQ-R**2)/(2.0*RO)
      A=ATAN(SQRT(1.0/COSA**2-1.0))
```

```
      IF (SIN(F+2.0*PI-2.0*PI*T))    1,1,2
    1 A=-A
    2 CONTINUE
      SINSI=(1.0+E*COS(F))/SQRT(1.0+2.0*E*COS(F)+E**2)
      COSSI=SQRT(1.0-SINSI**2)
      SI=ATAN(SINSI/COSSI)
      IF (PI-F)  3,4,4
    4 SI=PI-SI
    3 CONTINUE
      ALAMDA=PI/2.0+F+SI
      ERP=COS(ALAMDA-2.0*PI*T)
      ERQ=(-1.0)*SIN(ALAMDA-2.0*PI*T)
      ERZ=0.0
      EVELP=2.0*PI*SIN(ALAMDA-2.0*PI*T)
      EVELQ=2.0*PI*COS(ALAMDA-2.0*PI*T)
      EVELZ=0.0
      RP=R*SIN(SI)
      RQ=R*COS(SI)
      RZ=0.0
      VP=0.0
      VQ=V
      VZ=0.0
      ROP=RP-ERP
      ROQ=RQ-ERQ
      ROZ=0.0
      RODTP=VP-EVELP
      RODTQ=VQ-EVELQ
      RODTZ=0.0
      PHI=ALAMDA-2.0*PI*T
    5 CONTINUE
      IF (I-2) 7,8,9
    7 H(1)=1.0/RO*SIN(A-PHI)
      H(2)=2.0/RO*COS(A-PHI)
      H(3)=0.0
      H(4)=0.0
      H(5)=0.0
      H(6)=0.0
      GO TO 10
    8 CONTINUE
      H(1)=0.0
      H(2)=0.0
      H(3)=1.0/RO
      H(4)=0.0
      H(5)=0.0
      H(6)=0.0
      GO TO 10
    9 RODTR=RODTP*ROP+RODTQ*ROQ+RODTZ*ROZ
      H(1)=1.0/RO**3*(ROSQ*RODTP-RODTR*ROP)
      H(2)=1.0/RO**3*(ROSQ*RODTQ-RODTR*ROQ)
      H(3)=1.0/RO**3*(ROSQ*RODTZ-RODTR*ROZ)
      H(4)=ROP/RO
      H(5)=ROQ/RO
      H(6)=ROZ/RO
   10 RETURN
```

```
      END
/FTC     DECK
      SUBROUTINE PERI(N,EP)
      COMMON EX(6,6),SS(3),ST(30),E,AVN,EAP,F,PI,U,AM
      DIMENSION CI(6,6),CIT(6,6),EPI(6,6),H(6),HH(6,6),S(6,6),
     1B(6,6),TM(3,3),TN(3,3),TS(3,3),TT(3,3),EP(6,6),EO(6,6)
      DOUBLE PRECISION AA(6,6)
      DO 3 I=1,30
   34 FORMAT )/*
      WRITE )6,34*
      M1=0
      CALL CCOM (I,CI,CIT,TM,TN,TS,TT)
      DO 3 J=1,N
      CALL VCTR (I,J,H)
   93 FORMAT (6E18.9)
   51 FORMAT (2F30.15)
      WRITE (6,51) ST(I),F
      WRITE (6,93) (H(JJ),  JJ=1,6)
      CALL MPY1 (HH,H)
      CALL MPY2(B,HH,CI)
      CALL MPY3 (S,CIT,B)
      DO 3 K=1,6
      DO 3 L=K,6
    1 S(K,L)=S(K,L)/SS(J)
      AA(K,L)=S(K,L)+AA(K,L)
      IF (K-L) 2,3,2
    2 AA(L,K)=AA(K,L)
    3 CONTINUE
      CALL SUM (EPI,EX,AA)
      CALL NVRT (EP,EPI)
      DO 4 K=1,6
      DO 4 L=1,6
    4 AA(K,L)=0.0
      RETURN
      END
/FTC     DECK
      SUBROUTINE TRUE(ECC,EMA,TA,E)
C     COMPUTE THE TRUE ANOMALY FOR ELLIPTIC OR HYPERBOLIC ORBIT
C     GIVEN THE MEAN ANOMALY AND ECCENTRICITY
      TOL= 1.0E-06
      CONV= 57.29577957
      IF(ABS(EMA)-TOL)80,90,90
   80 E=0.
      TA=0.
      GO TO 18
   90 IF(ECC-.001)20,30,30
   20 ROOT=1.
      GO TO 40
   30 ROOT= SQRT ( ABS ( (1.+ ECC)/(1.- ECC) ) )
   40 E=EMA
      DO 10 I=1,10
      DE=(EMA-(E-ECC*SIN (E)))/(1.-ECC*COS (E))
      E= E+DE
      IF( ABS (DE/E)- TOL) 15,15,10
```

```
 10    CONTINUE
   15 TA=2.*ATAN(ROOT*SIN(E/2.)/COS(E/2.))
 18    RETURN
       END
/FTC      DECK
       SUBROUTINE CCOM (M,CI,CIT,TM,TN,TS,TT)
       COMMON EX(6,6),SS(3),ST(30),E,AVN,EAP,F,PI,U,AM
C      L=0 FOR CLUSTERS  L=1 FOR SAMPLES  M IS THE OPEN LOOP INDEX
       DIMENSION CI(6,6),CIT(6,6),TM(3,3),TN(3,3),TS(3,3),TT(3,3)
       IF (M) 2,2,1
     1 A=-PI+AVN*ST(M)
       CALL TRUE (E,A,F,EAC)
     4 CALL MTRM(TM,E,EAC,EAP,AVN)
       CALL MTRN(TN,E,EAC,EAP,AVN)
       CALL MTRS(TS,E,EAC,EAP,AVN)
       CALL MTRT(TT,E,EAC,EAP,AVN)
     2 DO 5 I=1,3
       DO 5 J=1,3
       CI(I,J)=TT(J,I)
       CI(I,J+3)=-TN(J,I)
       CI(I+3,J)=-TS(J,I)
       CI(I+3,J+3)=TM(J,I)
       CIT(I,J)=TT(I,J)
       CIT(I,J+3)=-TS(I,J)
       CIT(I+3,J)=-TN(I,J)
     5 CIT(I+3,J+3)=TM(I,J)
       RETURN
       END
/FTC      DECK
       SUBROUTINE MTRM(C,ECC,EAC,EAD,ANVEL)
       DIMENSION C(3,3)
       E=ECC
       X=EAC
       Y=EAD
       Z=(Y-X)/2.
       U=(Y+X)/2.
       T=(3.*Z-ECC*SIN (Z)*COS (U))*(COS (Z)+ECC*COS (U ))-4.*SIN (Z)
       B=ANVEL
       SNX=SIN (X)
       SNY=SIN (Y)
       SNZ=SIN (Z)
       SNU=SIN (U)
       CSX=COS (X)
       CSY=COS (Y)
       CSZ=COS (Z)
       CSU=COS (U)
       ALPHA=SQRT (1.0-E**2)
       BETA=1.0-E*CSY
       DELTA=1.0-E*CSX
       PHI=1.0+E*CSX
       TZI=1.0+E*CSY
       GAMMA=    SQRT ((1.-E**2*CSX**2)*      (1.-E**2*CSY**2))
       C(1,1)=(      (PHI*BETA+((2.*SNZ*BETA)/DELTA**2)*((1.-E**2)
      1*SNZ-DELTA*E*SNX*CSZ)))/GAMMA
```

```
      C(1,2)=(      ((2.*ALPHA*BETA)/DELTA**2)*SNZ*(CSZ-E*CSU))/GAMMA
      C(1,3)=0.0
      C(2,1)=(((      2.*ALPHA)/DELTA**2)*((-TZI)*(3.*Z-E*SNZ*CSU)+2.
     1*SNZ*(E*CSU+CSZ*(1.0+E*CSX-E**2*CSX**2))))/GAMMA
      C(2,2)=      ((DELTA*TZI+(2.0/DELTA**2)*((-TZI)*E*SNX*(3.*Z-E*SNZ
     1*CSU)+2.0*SNZ*(2.0*E*SNU-(1.0+E**2)*SNZ)))  )/GAMMA
      C(2,3)=0.0
      C(3,1)=0.0
      C(3,2)=0.0
      C(3,3)=1.-((2.*SNZ**2)/DELTA)
      RETURN
      END
/FTC     DECK
      SUBROUTINE MTRN(F,ECC,EAC,EAD,ANVEL)
      DIMENSION F(3,3)
      E=ECC
      BETA=2./ANVEL
      X=EAC
      Y=EAD
      Z=(Y-X)/2.
      U=(Y+X)/2.
      T=(3.*Z-ECC*SIN (Z)*COS (U))*(COS (Z)+ECC*COS (U ))-4.*SIN (Z)
      SNX=SIN (X)
      SNY=SIN (Y)
      SNZ=SIN (Z)
      SNU=SIN (U)
      CSX=COS (X)
      CSY=COS (Y)
      CSZ=COS (Z)
      CSU=COS (U)
      ALPHA=SQRT (1.0-E**2)
      GAMMA=BETA/(SQRT (1.-E**2*CSX**2)*SQRT (1.-E**2*CSY**2))
      PHI=1.0-E*CSX
      TZI=1.0-E*CSY
      F(1,1)=GAMMA*PHI*TZI*SNZ*(CSZ+E*CSU)
      F(1,2)=GAMMA*2.0*ALPHA*TZI*SNZ**2
      F(1,3)=0.0
      F(2,1)=-(GAMMA*2.*ALPHA*PHI*SNZ**2)
      F(2,2)=GAMMA*(4.*SNZ*(CSZ+E*CSU)-(1.+E*CSX)*(1.+E*CSY)*(3.*Z-
     1E*SNZ*CSU))
      F(2,3)=0.0
      F(3,1)=0.0
      F(3,2)=0.0
      F(3,3)=BETA*SNZ*(CSZ-E*CSU)
      RETURN
      END
/FTC     DECK
      SUBROUTINE MTRS(S,ECC,EAC,EAD,ANVEL)
      DIMENSION S(3,3)
      E=ECC
      X=EAC
      Y=EAD
      Z=(Y-X)/2.
      U=(Y+X)/2.
```

```
      T=(3.*Z-ECC*SIN (Z)*COS (U))*(COS (Z)+ECC*COS (U ))-4.*SIN (Z)
      SNX=SIN (X)
      B=ANVEL
      SNY=SIN (Y)
      SNZ=SIN (Z)
      SNU=SIN (U)
      CSX=COS (X)
      CSU=COS (U)
      CSZ=COS (Z)
      CSY=COS (Y)
      BETA=1.0-E*CSX
      ALPHA=1.0-E**2
      DELTA=1.0-E*CSY
      GAMMA=(2.0*B)/(BETA**2*DELTA**2*SQRT (1.0-E**2*CSX**2)*SQRT (1.0-E
     1**2*CSY**2))
      S(1,1)=GAMMA*(ALPHA*(3.0*Z-2.0*E*SNZ*CSU)-(BETA*DELTA*E**2*SNX*
     1SNY+ALPHA*(1.0+BETA*E*CSX+E*CSY*DELTA))*SNZ*CSZ)
      S(1,2)=GAMMA*SQRT (ALPHA)*(3.0*E*SNX*(Z-E*SNZ*CSU)+SNZ**2*(ALPHA+E
     1*CSY*DELTA)-E**2*SNZ*SNU*(2.0*BETA*CSZ*CSU+CSY*DELTA))
      S(1,3)=0.0
      S(2,1)=GAMMA*SQRT (ALPHA)*(3.0*E*SNY*(Z-E*SNZ*CSU)-SNZ**2*(ALPHA
     1+E* CSX*BETA)-E**2*SNZ*SNU*(2.0*DELTA*CSZ*CSU+CSX*BETA))
      S(2,2)=GAMMA*(E**2*SNX*SNY*(3.0*Z-4.0*E*SNZ*CSU+E**2*SNZ*CSZ*(CSU*
     1*2-SNU**2))-ALPHA*SNZ*(CSZ*(1.0+E**2)-2.0*E*CSU))
      S(2,3)=0.0
      S(3,1)=0.0
      S(3,2)=0.0
      S(3,3)=-(2.*B*((SNZ*CSZ)/(BETA*DELTA)))
      RETURN
      END
/ETC     DECK
      SUBROUTINE MTRT(T,ECC,EAC,EAD,ANVEL)
      DIMENSION T(3,3)
      E=ECC
      X=EAC
      Y=EAD
      Z=(Y-X)/2.
      U=(Y+X)/2.
      B=ANVEL
      SNX=SIN (X)
      SNY=SIN (Y)
      SNZ=SIN (Z)
      SNU=SIN (U)
      CSX=COS (X)
      CSY=COS (Y)
      CSZ=COS (Z)
      CSU=COS (U)
      ALPHA=1.0-E**2
      BETA=1.0-E*CSX
      DELTA=1.0-E*CSY
      PHI=1.0+E*CSX
      TZI=1.0+E*CSY
      GAMMA=    SQRT ((1.-E**2*CSX**2)*      (1.-E**2*CSY**2))
      T(1,1)=      ((TZI*BETA+((2.*SNZ*BETA)/DELTA**2)*(ALPHA*SNZ+DELTA
```

```
     1*E*SNY*CSZ)))/GAMMA
      T(1,2)=(((      2.*SQRT (ALPHA))/DELTA**2)*(PHI*(3.*Z-E*SNZ*CSU)
     1-2.0*SNZ*(E*CSU+CSZ*(TZI-E**2*CSY**2))))/GAMMA
      T(1,3)=0.0
      T(2,1)=-((      (((2.*SQRT (ALPHA)*BETA)/DELTA**2)*SNZ*(CSZ-E*CSU
     1))))/GAMMA
      T(2,2)=(      (DELTA*PHI+(2.0/DELTA**2)*(PHI*E*SNY*(3.0*Z-E*SNZ
     1*CSU)-2.0*SNZ*(2.0*E*SNU+SNZ*(1.0+E**2)))))/GAMMA
      T(2,3)=0.0
      T(3,1)=0.0
      T(3,2)=0.0
      T(3,3)=1.-((2.*SNZ**2)/DELTA)
      RETURN
      END
/FTC      DECK
      SUBROUTINE XTRP (EO,EAC)
C     XTRP EXTRAPOLATES INITIAL COVARIANCE MATRIX(EO) FROM INITIAL
C     POINT(EAC/HAC) TO PERI-POINT
      COMMON EX(6,6),SS(3),ST(3),E,AVN,EAP,F,PI,U,AM
      DIMENSION EO(6,6),EOI(6,6),CI(6,6),CIT(6,6),A(6,6),TM(3,3),TN(3,3)
     1,TS(3,3),TT(3,3)
    1 CALL MTRM(TM,E,EAC,EAP,AVN)
      CALL MTRN(TN,E,EAC,EAP,AVN)
      CALL MTRS(TS,E,EAC,EAP,AVN)
      CALL MTRT(TT,E,EAC,EAP,AVN)
      CALL CCOM (0,CI,CIT,TM,TN,TS,TT)
      CALL NVRT(EOI,EO)
      CALL MPY2(A,EOI,CI)
      CALL MPY3(EX,CIT,A)
      RETURN
      END
/FTC      DECK
      SUBROUTINE NVRT(QQ,QQQ)
C     INVERSION OF 6X6 MATRIX
      DOUBLE PRECISION Q(6,12),S,DIV
      DIMENSION QQ(6,6),QQQ(6,6)
      DO 10 I=1,6,1
      DO 5 J=1,6,1
      Q(I,J)=QQQ(I,J)
    5 Q(I,J+6)=0.000000000
   10 Q(I,I+6)=1.000000000
      DO 30 I=1,6,1
      DO 14 J=I,6,1
      IF(DABS(Q(I,I))-DABS(Q(J,I)))11,14,14
   11 DO 12 K=1,6,1
      S=Q(J,K)
      Q(J,K)=Q(I,K)
      Q(I,K)=S
      S=Q(J,K+6)
      Q(J,K+6)=Q(I,K+6)
   12 Q(I,K+6)=S
   14 CONTINUE
      DIV=Q(I,I)
      DO 15 J=1,6,1
```

```
      Q(I,J)=Q(I,J)/DIV
   15 Q(I,J+6)=Q(I,J+6)/DIV
      DO 30 J=1,6,1
      IF (I-J) 20,30,20
   20 DIV=Q(J,I)
      DO 25 K=1,6,1
      Q(J,K)=Q(J,K)-Q(I,K)*DIV
   25 Q(J,K+6)=Q(J,K+6)-Q(I,K+6)*DIV
   30 CONTINUE
      DO 35 I=1,6,1
      DO 35 J=1,6,1
   35 QQ(I,J)=Q(I,J+6)
      RETURN
      END
/FTC     DECK
      SUBROUTINE MPY1(HH,H)
C     INDEXED VECTOR TIMES ITS TRANSPOSE
      DOUBLE PRECISION A(6)
      DIMENSION H(6),HH(6,6)
      DO 1 I=1,6
    1 A(I)=H(I)
      DO 3 I=1,6
      DO 3 J=I,6
      HH)I,J*=A)I**A)J*
      IF)I-J*2,3,2
    2 HH)J,I*=HH)I,J*
    3 CONTINUE
      RETURN
      END
/FTC     DECK
      SUBROUTINE MPY2(XX,XY,XZ)
C     XY TIMES XZ
      DOUBLE PRECISION A)6,6*,B)6,6*,C)6,6*
      DIMENSION XX(6,6),XY(6,6),XZ(6,6)
      DO 2 J=1,6
      DO 2 K=1,6
      A)J,K*=XY)J,K*
    2 B)J,K*=XZ)J,K*
      DO 1 J=1,6
      DO 1 K=1,6
      C)J,K*=0.
      DO 1 L=1,6
    1 C)J,K*=C)J,K*.A)J,L**B)L,K*
      DO 3 J=1,6
      DO 3 K=1,6
    3 XX)J,K*=C)J,K*
      RETURN
      END
/FTC     DECK
      SUBROUTINE MPY3(XX,XY,XZ)
C     XY TIMES XZ, XX IS SYMMETRIC
      DOUBLE PRECISION A)6,6*,B)6,6*,C)6,6*
      DIMENSION XX(6,6),XY(6,6),XZ(6,6)
      DO 4 J=1,6
```

```
      DO 4 K=1,6
      A)J,K*=XY)J,K*
    4 B)J,K*=XZ)J,K*
      DO 3 J=1,6,1
      DO 3 K=J,6,1
      C)J,K*=0.
      DO 3 L=1,6,1
      C)J,K*=C)J,K*+A)J,L**B)L,K*
      IF (L-6) 3,1,1
    1 IF (J-K) 2,3,2
    2 C)K,J*=C)J,K*
    3 CONTINUE
      DO 5 J=1,6
      DO 5 K=1,6
    5 XX)J,K*=C)J,K*
      RETURN
      END
/FTC     DECK
      SUBROUTINE SUM)ZX,ZY,C*
C     ZY+ZZ, ZX IS SYMMETRIC
      DOUBLE PRECISION A)6,6*,B)6,6*,C)6,6*
      DIMENSION ZX)6,6*,ZY)6,6*
      DO 3 I=1,6
      DO 3 J=1,6
    3 B)I,J*=ZY)I,J*
      DO 2 J=1,6,1
      DO 2 K=J,6,1
      A)J,K*=B)J,K*+C)J,K*
      IF (J-K) 1,2,1
    1 A)K,J*=A)J,K*
    2 CONTINUE
      DO 4 I=1,6
      DO 4 J=1,6
    4 ZX)I,J*=A)I,J*
      RETURN
      END


/DATA
  .02000.05000.10000.18000.22000.280
  .30000.32000.35000.38000.40000.420
  .45000.48000.50000.52000.58000.600
  .62000.64000.70000.75000.78000.800
  .82000.85000.88000.90000.94000.960
+.107010000E-06+.107010000E-06+.107010000E-06
+.153300000E-02+.290270000E-03+.153300000E-02
+.304000000E-05+.304000000E-05+.399000000E-02
+.304000000E-05+.304000000E-05+.177400000E-02
+.304000000E-05+.304000000E-05+.444000000E-03
+.304000000E-05+.304000000E-05+.160000000E-03
+.304000000E-05+.304000000E-05+.400000000E-04
+.304000000E-05+.304000000E-05+.444000000E-05
+.304000000E-05+.304000000E-05+.400000000E-06
```

```
+.304000000E-05+.304000000E-05+.160000000E-07
+.304000000E-03+.304000000E-03+.160000000E-07
+.304000000E-05+.304000000E-05+.400000000E-08
+.304000000E-05+.304000000E-05+.160000000E-09
+.304000000E-05+.304000000E-05+.400000000E-10
/END OF FILE
```

APPENDIX B

DERIVATIONS PERTAINING TO THE MEASUREMENT VECTORS

B.1 Justification of Equation 3.5

Any measurement quantity can be written as some scalar function of the probe state.

$$m = f(\underline{x}) \tag{B.1}$$

The exact functional form of $f(\underline{x})$ depends upon the quantity measured. However, at this point we are not interested in the particular functional form, but rather, the same relationship does exist. At any specified time, the relation can be written for the nominal state and also for any other point in the state space. If the non-nominal point is in the region of convergence of a Taylor Series, then equation B.1 can be expanded about the nominal state.

$$m = m_N + \frac{\partial f}{\partial \underline{x}}(\underline{x} - \underline{x}_N) + \frac{1}{2}(\underline{x} - \underline{x}_N)^T \left\{ \frac{\partial}{\partial \underline{x}} \left[\frac{\partial f}{\partial \underline{x}} \right]^T \right\} (\underline{x} - \underline{x}_N) + \ldots \tag{B.2a}$$

where the convention will be that

(B.2b)

If the state deviation, $(\underline{x} - \underline{x}_N)$, is small, equation B.2a can be linearized by truncating second and higher order terms. Then, by defining

$$\underline{h}^T = \frac{\partial f(\underline{x})}{\partial \underline{x}} \tag{B.3}$$

and substituting equations B.3, 3.1, and 3.4 into the linearized form of equation B.2, the desired result is obtained.

$$\delta m = \underline{h}^T \delta \underline{x} \tag{B.4}$$

In practice, finding $\underline{h}$ by taking partial derivatives of $f(\underline{x})$ may be inconvenient, because $f(\underline{x})$ may be difficult to determine.

However, equation B.4 expresses the form of the desired result, and the measurement vector, $\underline{h}$, may be obtainable in some round-about fashion that requires no knowledge of $f(\underline{x})$.

B.2 Coordinate Systems

Three coordinate systems are useful in this problem.

a) Inertial, Sun-centered Coordinate System

This coordinate system is specified as the XYZ frame. The $\underline{1}_X$ vector lies in the ecliptic and points at aphelion of the probe's two body ellipse about the sun. Injection into this ellipse is assumed to occur at aphelion, at $t = 0$. The $\underline{1}_Y$ vector lies in the ecliptic and points in the direction of nominal probe velocity at aphelion. The $\underline{1}_Z$ vector is defined by

$$\underline{1}_Z = \underline{1}_X \times \underline{1}_Y \qquad \text{(B.5)}$$

b) Earth-centered, Rotating Coordinate System

This coordinate system is specified as the xyz frame. The $\underline{1}_y$ vector points in the instantaneous direction of earth velocity and lies in the ecliptic. The $\underline{1}_x$ vector lies in the ecliptic, perpendicular to $\underline{1}_y$, and in general approximately along the sun-earth line. Specifically, for this problem, the earth is assumed to be in circular orbit, so that $\underline{1}_x$ is exactly along with the sun-earth line. This assumption is justified elsewhere (pg. 14). The $\underline{1}_z$ vector coincides with that of the XYZ frame.

c) Flight Path Coordinate System

This coordinate system is specified as the pqu frame. The $\underline{1}_q$ vector points along the instantaneous probe velocity. The $\underline{1}_p$ vector lies in the plane of probe motion, is perpendicular to $\underline{1}_q$, and points outward from the center of attraction. The $\underline{1}_u$ direction is defined by

$$\underline{1}_u = \underline{1}_p \times \underline{1}_q \qquad \text{(B.6)}$$

This coordinate system is specialized by selection of a nominal trajectory. For this problem, the nominal trajectory will lie in the ecliptic, and so will $\underline{1}_p$ and $\underline{1}_q$. These coordinate systems are shown for the general case in Figure B.1, and for the nominal trajectory used in this analysis in Figure 3.1.

B.3 The Azimuth and Elevation Angle Measurement Vectors

The measurement vectors for angular measurements are more

readily developed in the xyz frame. Consequently, they are derived in that frame, and in section B.4 are rotated in to the pqu frame.

From Figure B.1, we can write, in the xyz frame,

$$\underline{R} = \underline{r} + \underline{\rho} = \underline{r} + \rho \begin{bmatrix} -\cos L \cos A \\ \cos L \sin A \\ \sin L \end{bmatrix} \tag{B.7}$$

Taking the first-order variation of equation B.7 with respect to azimuth angle change gives

$$\delta \underline{R} = \frac{\partial \underline{R}}{\partial A} \delta A = \frac{\partial \underline{r}}{\partial A} \delta A + \rho \begin{bmatrix} \cos L \sin A \\ \cos L \cos A \\ 0 \end{bmatrix} \delta A \tag{B.8}$$

However, the sun-earth radius vector, $\underline{r}$, is a function of time only, so that $\partial \underline{r}/\partial A$ is zero. Taking the dot product of equation B.8 with $\partial \underline{\rho}/\partial A$ and simplifying gives the desired measurement vector. (Note the angle measurements depend upon probe position only.)

$$\delta A = \underline{a}^T \delta \underline{x} \tag{B.9a}$$

$$\underline{a}^T = \left[\underline{a}_3^T \vdots \underline{0}_3^T \right] = \frac{1}{\rho \cos L} \left[\sin A, \cos A, 0 \vdots \underline{0}_3^T \right] \tag{B.9b}$$

An identical procedure for the elevation angle gives

$$\delta L = \underline{b}^T \delta \underline{x} \tag{B.10a}$$

$$\underline{b}^T = \left[\underline{b}_3^T \vdots \underline{0}_3^T \right] = \frac{1}{\rho} \left[\sin L \cos A, -\sin L \sin A, \cos L \vdots \underline{0}_3^T \right] \tag{B.10b}$$

B.4 Rotation into Flight Path Coordinate System

Figure 3.2 shows the orientation of the three coordinate systems, for the nominal trajectory in the ecliptic, at some arbitrary time. The three frames are aligned at t = 0, which is injection at aphelion into an heliocentric, elliptic orbit. The angle between $\underline{1}_x$ and $\underline{1}_\rho$ is $\lambda(t)$.

$$\lambda(t) = \pi/2 + f(t) + \psi_{(t)} \tag{B.11}$$

The flight path angle, Ψ, is given by equation 3.15 and f(t), the true anomaly, is found as a solution to Kepler's problem. (See
The angle between $\underline{1}_x$ and $\underline{1}_p$ becomes

$$\phi(t) = \lambda(t) - 2\pi t \tag{B.12}$$

because the earth is in circular orbit.
Then, from Figure 3.2, we can find a rotation matrix, M, such that

$$\underline{S}_{pqu} = M\underline{S}_{xyz} \tag{B.13}$$

where $\underline{S}$ is an arbitrary column vector and the subscript indicates the frame in which $\underline{S}$ is written.

$$M = \begin{bmatrix} \cos\phi & \sin\phi & 0 \\ -\sin\phi & \cos\phi & 0 \\ 0 & 0 & 1 \end{bmatrix} \tag{B.14}$$

Using M to transform $\underline{a}$ and $\underline{b}$, we find

$$\underline{k}_3^T = \underline{a}_3^T M^T \tag{B.15a}$$

$$\underline{d}_3^T = \underline{b}_3^T M^T \tag{B.15b}$$

The result of the indicated operation, with $L = 0$ for the nominal case, is

$$\underline{k}^T = \frac{1}{\rho}\left[\sin(A-\phi)\ \cos(A-\phi)\ 0 \vdots \underline{0}_3^T\right] \tag{B.16a}$$

$$\underline{d}^T = \left[0\ 0\ \frac{1}{\rho} \vdots \underline{0}_3^T\right] \tag{B.16b}$$

B.5 The Range-Rate Measurement Vector

From Figure B.1 we can write

$$\underline{R} = \underline{r} + \underline{\rho} \tag{B.17}$$

Differentiation of equation B.17 yields

$$\underline{V} = \underline{v} + \dot{\underline{\rho}} \tag{B.18}$$

Solving equation B.18 for range-rate yields

$$\dot{\rho} = \dot{\underline{\rho}} \cdot \frac{\underline{\rho}}{\rho} = (\underline{V} - \underline{v}) \cdot \frac{\underline{\rho}}{\rho} \tag{B.19}$$

Then, for small deviations

$$\delta\dot{\rho} = \frac{\underline{\rho}}{\rho} \cdot \delta\dot{\underline{\rho}} + \dot{\underline{\rho}} \cdot \delta\left(\frac{\underline{\rho}}{\rho}\right) \tag{B.20}$$

Using the facts that

$$\rho^2 = \underline{\rho} \cdot \underline{\rho} \quad \text{and} \quad \delta\rho = \frac{\underline{\rho} \cdot \delta\underline{\rho}}{\rho} \tag{B.21}$$

we can simplify equation B.20 to get

$$\delta\dot{\rho} = \frac{\underline{\rho}}{\rho} \cdot \delta\dot{\underline{\rho}} + \left[\frac{(\underline{\rho} \cdot \underline{\rho})\dot{\underline{\rho}} - (\underline{\rho} \cdot \dot{\underline{\rho}})\underline{\rho}}{\rho^3}\right] \cdot \delta\underline{\rho} \tag{B.22}$$

Because the earth's position and velocity are known quantities, they are not subject to variation. Consequently,

$$\delta\underline{\rho} = \delta\underline{R} \quad \text{and} \quad \delta\dot{\underline{\rho}} = \delta\underline{V} \tag{B.23}$$

Substitution of equations B.23 into equation B.22 gives the desired result.

$$\delta\dot{\rho} = \underline{c}^T \delta\underline{x} \tag{B.24a}$$

where

$$\underline{c} = \begin{bmatrix} \dfrac{(\underline{\rho} \cdot \underline{\rho})\dot{\underline{\rho}} - (\underline{\rho} \cdot \dot{\underline{\rho}})\underline{\rho}}{\rho^3} \\ \underline{\rho}/\rho \end{bmatrix} \tag{B.24b}$$

Notice that nowhere has a coordinate system been specified, so that equation B.24a is valid as long as $\underline{c}^T$ and $\delta\underline{x}$ are coordinatized in the same system.

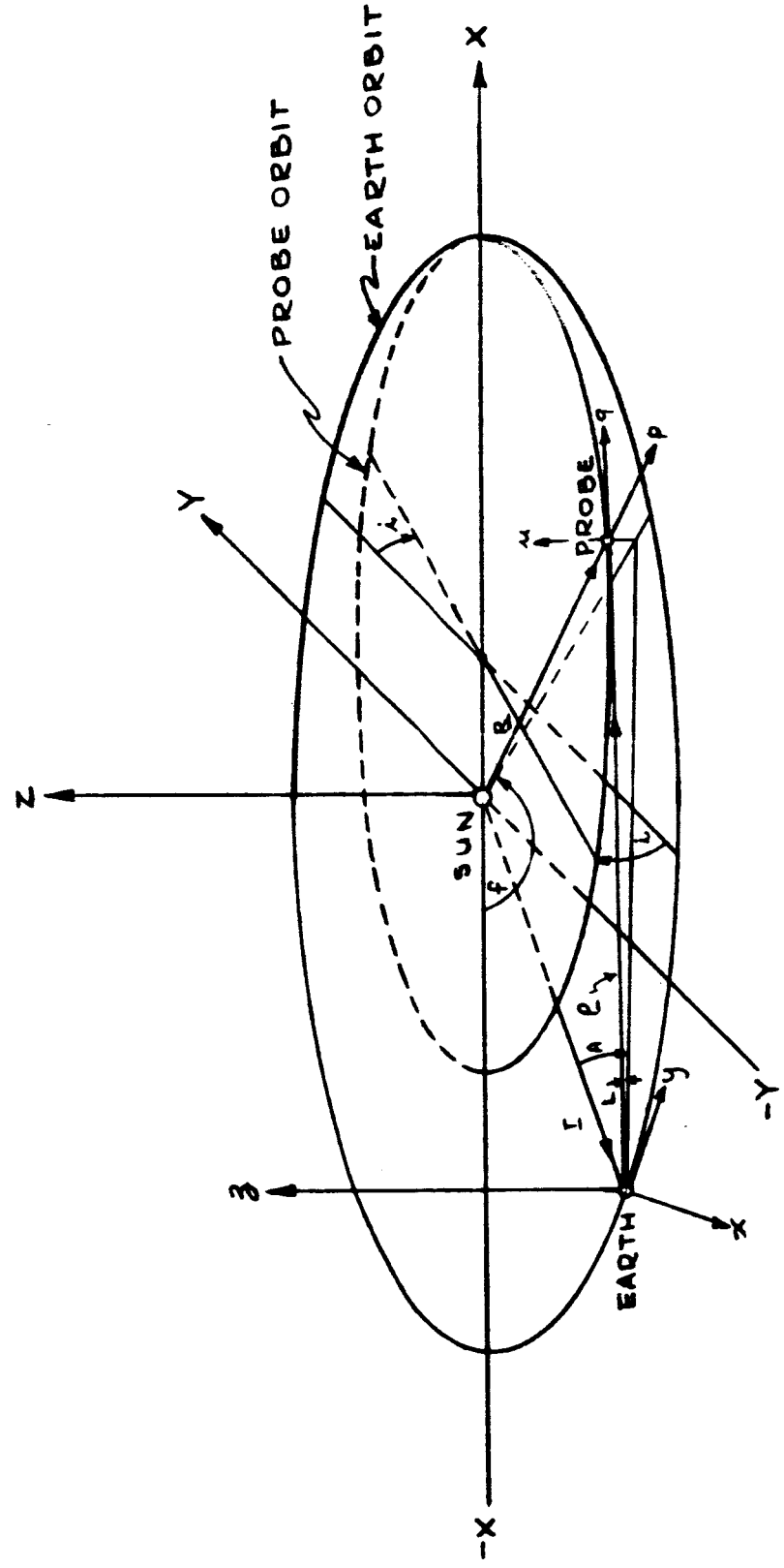

FIG. B.1

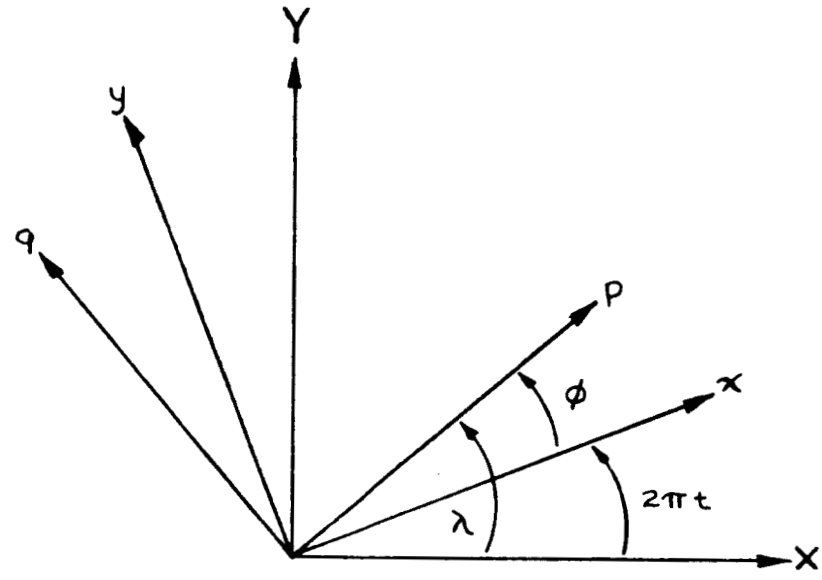

FIG. B.2

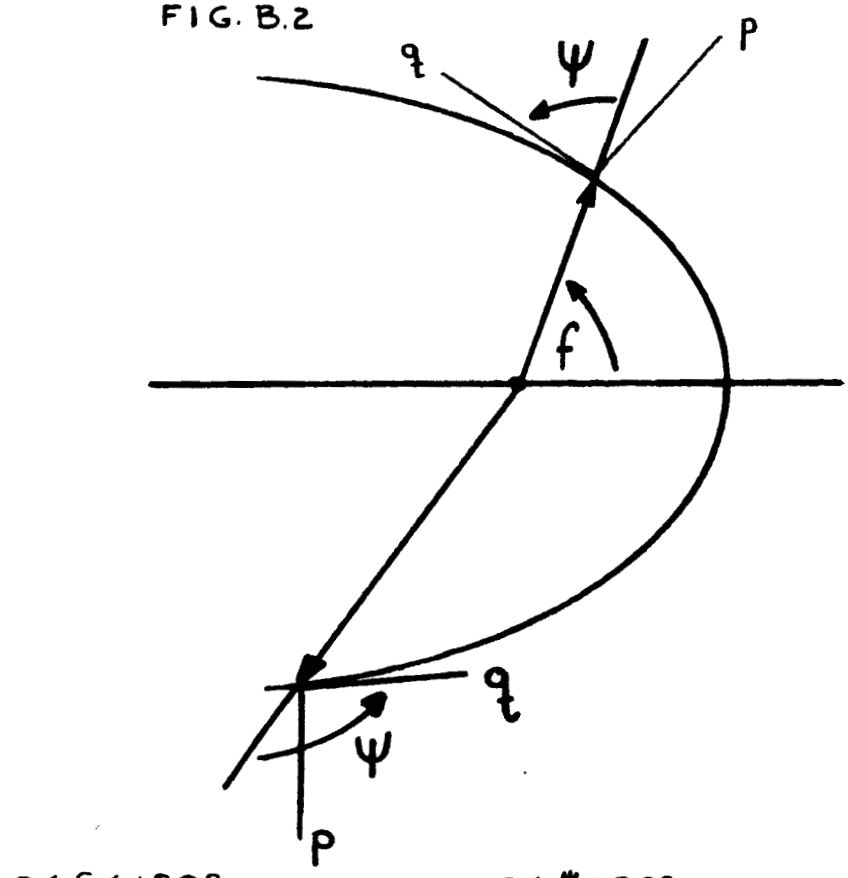

$0 \leq f \leq 180°$
$180° \leq f \leq 360°$

$0 < \psi \leq 90°$
$90° \leq \psi < 180°$

FIG. B3

APPENDIX C

CALCULATION OF VARIANCES AT THE SPHERE OF INFLUENCE

C.1 Variance in Position Components

As stated in Chapter 4, the LTV Astronautics Division conducted an error analysis on the launch vehicle for Sunblazer probe. ( ) In this analysis, nineteen separate error sources were identified and a Monte Carlo technique was used to extrapolate the errors to the sphere of influence. It is found that errors at the sphere of influence are normally distributed. In the analysis, the three sigma deviation in the magnitude of aphelion radius is 0.0017 AU about the nominal value of 1 AU. It is assumed here that the distributions of the deviations in all three components of aphelion radius are identical. Then,

$$\sigma_{Rq} = \sigma_{Rp} = \sigma_{Ru} \tag{C.1}$$

$$\sigma_R^2 = 3\sigma_{Rp}^3 \tag{C.2}$$

$$\sigma_{Rp} = \frac{1}{\sqrt{3}} \sigma_R \tag{C.3}$$

But,

$$\sigma_R = \frac{0.0017}{3} = 5.67 \times 10^{-4} \text{ AU} \tag{C.4a}$$

so that,

$$\sigma_{Rp} = 3.27 \times 10^{-4} \text{ AU} \tag{C.4b}$$

and

$$\sigma_{Rp}^2 = \sigma_{Rq}^2 = \sigma_{Ru}^2 = 10.7 \times 10^{-8} (\text{AU})^2 \tag{C.5}$$

Since injection occurs at aphelion, the variances in position components are given by equation C.5.

C.2 Variances in Velocity Components ($\underline{l}_p$ and $\underline{l}_u$ directions)

At nominal injection the probe velocity lies in the ecliptic and is perpendicular to the sun-probe line. The magnitude of nominal velocity can be obtained from

$$V_N^2 = \mu_s \left[\frac{2}{R} - \frac{1}{a}\right] \tag{C.6}$$

$$V_N = 81,320 \text{ ft/sec} \tag{C.7}$$

The LTV error analysis gives the standard deviation of the inclination angle as 0.44^o. Any velocity out of the plane of the ecliptic due to non-zero inclination angle constitutes a velocity deviation in the $\underline{l}_u$ direction. Both velocity pointing errors and magnitude errors contribute to velocity deviations in the $\underline{l}_u$ direction. However, the contribution of the magnitude errors is small compared to the contribution of the inclination errors. Consequently, the standard deviation of the velocity errors out of the ecliptic plane is

$$\sigma_{Vu} = V_N \sigma_i \tag{C.8}$$

$$\sigma_{Vu} = 3.92 \times 10^{-2} \text{ AU/yr.} = 609 \text{ ft/sec} \tag{C.9}$$

At nominal injection, the flight path angle is 90^o. Consequently, any non-zero velocity in the $\underline{l}_p$ direction at injection constitutes a deviation. It is assumed that the deviations in flight path angle are distributed in a fashion identical to the inclination angle deviations. Again, magnitude deviations contribute no appreciable error. Therefore,

$$\sigma_{Vp} = 3.92 \times 10^{-2} \text{ AU/yr.} \tag{C.10}$$

$$\sigma_{Vp}^2 = \sigma_{Vu}^2 = 15.33 \text{ (AU/yr)}^2 \times 10^{-4} \tag{C.11}$$

Equation C.11 gives the variances in velocity deviations in the $\underline{l}_p$ and $\underline{l}_u$ directions.

C.3 Variance in Velocity ($\underline{l}_q$ direction)

Nominal burnout occurs at an altitude of 1.05758×10^6 feet and a velocity of 39.2881×10^3 ft/sec with respect to the earth. The probe then coasts along a two-body (earth-probe) escape hyperbola to the

sphere of influence. Using burnout conditions and

$$V_h^2 = \mu_e \left[\frac{2}{r} + \frac{1}{a_h} \right] \tag{C.12}$$

one can compute the nominal semi-major axis as 0.54×10^8 ft and the nominal velocity at the sphere of influence of 16.42×10^4 ft/sec with respect to the earth. This velocity is oriented in the plane of the ecliptic and perpendicular to the sun-probe line.

The standard deviation of burnout velocities is 110 ft/sec. Taking the non-nominal burnout velocity as the nominal plus one standard deviation, and propogating this along an escape hyperbola ($a = 0.523 \times 10^8$ ft) to the sphere of influence yields a velocity magnitude at injection of 16.683×10^3 ft/sec. In this calculation, deviations in burnout altitude were not considered.

Pointing errors do not appreciably change the velocity vector in either magnitude or direction. Consequently, $(16.683 - 16.42) \times 10^3$ ft/sec is taken as the standard deviation in the $\underline{l}_q$ direction.

$$\sigma^2_{V_q} = 2.9 \times 10^{-4} \, (\mathrm{AU/yr})^2 \tag{C.13}$$

Equation C.13 gives the variance in the third velocity component.

APPENDIX D

DERIVATION OF THE MAXIMUM LIKELIHOOD FILTER

D.1 Useful Relationships

These relationships will be of use in the derivation that follows.

$$\delta \underline{m}_n = \begin{bmatrix} \underline{k}_n^T \\ \underline{d}_n^T \\ \underline{c}_n^T \end{bmatrix} \delta \underline{x}_n = H_n \delta \underline{x}_n \tag{D.1}$$

$$\delta \underline{\tilde{m}}_n' = H_n \delta \underline{\hat{x}}_n' \tag{D.2}$$

$$\delta \underline{m}_n = \delta \underline{m}_n + \begin{bmatrix} \alpha \\ \beta \\ \gamma \end{bmatrix} = \delta \underline{m}_n + \underline{\mu}_n \tag{D.3}$$

$$\delta \underline{\hat{x}}_n' = \Phi_{n,n-1} \delta \underline{\hat{x}}_{n-1} = \delta \underline{x}_n + \underline{e}_n' \tag{D.4}$$

$$\delta \underline{\hat{x}}_n = \delta \underline{x}_n + \underline{e}_n \tag{D.5}$$

$$\underline{e}_n' = \Phi_{n,n-1} \underline{e}_{n-1} \tag{D.6}$$

D.2 The Optimum Filter

The recursive estimation procedure is formulated as

$$\delta \underline{\hat{x}}_n = \delta \underline{\hat{x}}_n' + W_n [\delta \underline{\tilde{m}}_n - \delta \underline{\tilde{m}}_n'] \tag{D.7}$$

Substitution of equations D.2 through D.5 into D.7 yields

$$\delta \underline{x}_n + \underline{e}_n = \delta \underline{x}_n + \underline{e}_n' + W_n [\delta \underline{m}_n + \underline{\mu}_n - H_n (\delta \underline{x}_n + \underline{e}_n')] \tag{D.8}$$

This reduces to

$$\underline{e}_n = \underline{e}_n' + W_n[\underline{\mu}_n - H_n\underline{e}_n'] = [I - W_nH_n]\underline{e}_n' + W_n\underline{\mu}_n \tag{D.9}$$

From equation D.9 write $\overline{\underline{e}\,\underline{e}^T}$, the error covariance matrix.

$$\overline{\underline{e}_n\underline{e}_n^T} = E_n = (I - W_nH_n)\overline{\underline{e}_n'\underline{e}_n'^T}(I - W_nH_n)^T + W_n\overline{\underline{\mu}_n\underline{\mu}_n^T}W_n \tag{D.10}$$

Note that the cross product terms (e.g., $\overline{\underline{e}_n'\underline{\mu}_n^T}$) are zero because the measurement errors at t_n, $\underline{\mu}_n$, are independent of the updated error vector, $\underline{e}_n'$, and have zero mean value. Then,

$$E_n = (I - W_nH_n)E_n'(I - W_nE_n)^T + W_nA_nW_n^T \tag{D.11}$$

Recalling that the trace of E is a quadratic function of $\underline{e}$, we can write

$$\overline{e^2} = \mathrm{tr}[E_n] \tag{D.12}$$

Then, a necessary condition for a minimum mean squared error, $\overline{e^2}$, is that the first variation of equation D.12 with respect to W_n be zero. This will supply us with a relationship that the optimum filter must satisfy. Furthermore, if this filter can be shown to meet sufficient conditions, then it is an optimum filter and a maximum likelihood filter, because it minimizes a quadratic function of $\underline{e}$.

$$\delta\overline{e_n^2} = \mathrm{tr}[-\delta W_nH_nE_n'(I - W_nH_n)^T - (I - W_nH_n)E_n'H_n^T\delta W_n^T + \delta W_n A_n W_n^T + W_nA_n\delta W_n^T] \tag{D.13}$$

But

$$\mathrm{tr}[B] = \mathrm{tr}[B^T] \tag{D.14}$$

so that

$$\delta\overline{e_n^2} = -2\mathrm{tr}[\delta W_nH_nE_n'(I - W_nH_n)^T - \delta W_nA_nW_n^T] = 0 \tag{D.15}$$

$$0 = \mathrm{tr}\left\{\delta W_n[H_nE_n'(I - W_nH_n)^T - A_nW_n^T]\right\} \tag{D.16}$$

If W_n is a true optimum filter, equation D.16 must be true for arbitrary (small) δW_n. This is guaranteed if

$$[H_nE_n'(I - W_nH_n)^T - A_nW_n^T] = 0 \tag{D.17}$$

Solving equation D.17 for W_n^o yields a filter that meets necessary conditions.

$$W_n^{oT} = [H_n E'_n H_n^T + A_n]^{-1} H_n E'_n \tag{D.18}$$

To prove W_n^o is sufficient for a minimum $\overline{e^2}$, in equation D.11 substitute $W_n^o + \delta W_n$ for W_n.

$$E_n = (I - W_n^o H_n - \delta W_n H_n) E'_n (I - W_n^o H_n - \delta W_n H_n)^T + (W_n^o + \delta W_n) A_n (W_n^o + \delta W_n)^T \tag{D.19}$$

Expanding and taking the trace yields

$$\begin{aligned}
tr[E_n] = tr[&(I - W_n^o H_n) E'_n (I - W_n^o H_n)^T - (I - W_n^o H_n) E'_n H_n \delta W_n^T \\
&- \delta W_n H_n E'_n (I - W_n^o H_n)^T + \delta W_n H_n E'_n H_n^T \delta W_n^T \\
&+ W_n^o A_n W_n^{oT} + \delta W_n A_n \delta W_n^T \\
&+ \delta W_n A_n W_n^{oT} + W_n^o A_n \delta W_n^T] \\
= tr[&(I - W_n^o H_n) E'_n (I - W_n^o H_n)^T + W_n^o A_n W_n^{oT}] \\
&-2tr[\delta W_n H_n E'_n (I - W_n^o H_n)^T - \delta W_n A_n W_n^o] \\
&+ tr[\delta W_n (H_n E'_n H_n^T + A_n] \delta W_n^T] \\
= tr[E_n^o] &+ tr[\delta W_n (H_n E'_n H_n^T + A_n) \delta W_n^T] \\
&- 2tr[\delta W_n (H_n E'_n - H_n E'_n H_n^T W_n^{oT} - A_n W_n^T)] \\
= tr[E_n^o] &+ tr[\delta W_n (H_n E'_n H_n^T + A_n) \delta W_n^T] \\
&- 2tr[\delta W_n (\{H_n E'_n H_n^T + A_n\} W_n^{oT} - \{H_n E'_n H_n^T + A_n\} W_n^{oT}]
\end{aligned}$$

$$tr[E_n] = tr[E_n^o] + tr[\delta W_n (H_n E'_n H_n^T + A_n) \delta W_n^T] \tag{D.20}$$

Here, the quantity $tr[E_n^o]$ is recognized as the result of inserting only W_n^o in to equation D.11. Also, the second term can be rearranged.

$$\text{2nd term} = tr[\delta W_n^T \delta W_n (H_n E'_n H_n^T + A_n)] \tag{D.21}$$

Both $\delta W_n^T \delta W_n$ and $(H_n E'_n H_n^T + A_n)$ are positive definite, 3×3 matrices,

so that their product is positive definite. A property of a positive definite matrix is that its trace is positive. Consequently, it is evident from equation D. 20 that using any filter other than W_n^o produces a mean squared error that is larger than that produced by the W_n^o. Therefore, W_n^o also satisfies a sufficient condition and the optimum filter is W_n^o.

Substitution of W_n^o into equation D. 11 yields a recursion formula for E.

$$E_n = (I - W_n^o H_n) E'_n (I - W_n^o H_n)^T + W_n^o A_n W_n^{oT}$$

$$E_n = E'_n - W_n^o H_n E'_n - E'_n H_n^T W_n^{oT} + W_n^o H_n E'_n H_n^T W_n^{oT} + W_n^o A_n W_n^{oT}$$

$$= E'_n - E'_n H_n^T (H_n E'_n H_n^T + A_n)^{-1} H_n E'_n - E'_n H_n^T (H_n E'_n H_n^T + A_n)^{-1} H_n E'_n + W_n^o (H_n E'_n H_n^T + A_n) W_n^{oT}$$

$$= E'_n - 2E'_n H_n^T W_n^{oT} + E'_n H_n^T (H_n E'_n H_n^T + A_n)^{-1} (H_n E'_n H_n^T + A_n) W_n^{oT}$$

$$E_n = E'_n - E'_n H_n^T W_n^{oT} \qquad \text{(D. 22)}$$

Then, the result of this derivation is a maximum likelihood filter which is usable in the following recursive formulas.

$$\delta \underline{\hat{x}}_n = \delta \underline{\hat{x}}'_n + W_n^{oT} (\delta \underline{\tilde{m}}_n - H_n \delta \underline{\hat{x}}'_n) \qquad \text{(D. 23)}$$

$$E_n = E'_n - E'_n H_n^T W_n^{oT} \qquad \text{(D. 24)}$$

$$W_n^{oT} = (H_n E'_n H_n^T + A_n)^{-1} H_n E'_n \qquad \text{(D. 25)}$$

D. 3 Alternate Recursion Relation for E_n

Hypothesize that the following method of determining the error covariance matrix at time t_n is valid.

$$E_n^{-1} = E'^{-1}_n + H_n^T A_n^{-1} H_n \qquad \text{(D. 26)}$$

Use the matrix identity (Ref. 3)

$$(F_{nn} + B_{nm} C_{mm}^{-1} B_{mn})^{-1}$$

$$= F_{nn}^{-1} - F_{nn}^{-1} B_{nm} (C_{mm} + B_{mn} F_{nn}^{-1} B_{nm})^{-1} B_{mn} F_{nn}^{-1} \qquad \text{(D. 27)}$$

where the subscripts define the dimensions of the matrices.

Define

$$E'^{-1}_n = F_{nn} \tag{D.28a}$$

$$B_{nm} = H^T_n \tag{D.28b}$$

$$C_{mm} = A_n \tag{D.28c}$$

Substitution of definitions D. 28 into equation D. 27 gives

$$(E'^{-1}_n + H^T_n A^{-1}_n H_n)^{-1} = E'_n - E'_n H^T_n (A_n + H_n E'_n H^T_n)^{-1} H_n E'_n \tag{D.29}$$

$$E_n = E'_n - E'_n H^T_n (A_n + H_n E'_n H^T_n)^{-1} H_n E'_n \tag{D.30}$$

Substitution of equation D. 25 into equation D. 24 yields

$$E_n = E'_n - E'_n H^T_n (A_n + H_n E'_n H^T_n)^{-1} H_n E'_n \tag{D.31}$$

The recursion relation developed earlier with the filter gives a result (D. 31) that is identical to the result obtained by taking the inverse of equation D. 26. Consequently, calculation of the error covariance matrix using equation D. 26 is completely equivalent to calculating it using equation D. 24.

REFERENCES

1. Baker, R.H., and others, Study of a Small Solar Probe, Part II, Center for Space Research, M.I.T., Cambridge, Mass., 1965.
2. Battin, Richard H., Astronautical Guidance, McGraw-Hill, Inc., New York, 1964.
3. Battin, Richard H., unpublished notes for course 16.46, Astronautical Guidance I, M.I.T., Cambridge, Mass., Fall, 1965-66.
4. Duetch, Ralph, Orbital Dynamics of Space Vehicles, Prentice-Hall, Inc., Englewood Cliffs, N.J., 1963.
5. Eschbach, Ovid W., ed., Handbook of Engineering Fundamentals, John Wiley and Sons, Inc., New York, 1952.
6. Fagan, John H., unpublished report, J.H. Fagan and James E. Potter, Experimental Astronomy Laboratory, to be published during the summer, 1966. The report is not yet named. The subject is optimum navigation measurements.
7. Halfman, Robert L., Dynamics: Systems Variational Methods, and Relativity, Vol. II, Addison-Wesley Publishing Co., Inc., Reading, Mass., 1962.
8. Harrington, J.V., Study of a Small Solar Probe, Part I, Center for Space Research, M.I.T., Cambridge, Mass., 1965.
9. Ling-Temco-Vought, Inc., Astronautics Division, Feasibility and Parametric Design Study of an Unguided Solid Fuel Rocket Vehicle with Solar Orbital Capabilities, Dallas, 1965.
10. Deleted
11. Potter, James E. and Robert G. Stern, Statistical Filtering of Space Navigation Measurements, RE-3, Experimental Astronomy Laboratory, M.I.T., Cambridge, Mass., 1963.
12. Stern, R.G., "Interplanetary Midcourse Guidance Analysis," Sc.D. thesis in Department of Aeronautics and Astronautics, M.I.T., May 1963.

13. McCoubrey, A. O., "A Survey of Atomic Frequency Standards," Proceedings of the IEEE, 54: 2, February, 1966.

14. Private discussion with two people; Mr. William Cooper of the Center for Space Research; and Mr. Theodore Saito, a physics graduate student (M. I. T.) whose thesis area is scattering phenomona.

(The following convention is used in documenting this paper. (X:XX) means page number XX of reference number X.